Rapid increase of observed DIC and pCO(2) in the surface waters of the North Sea in the 2001-2011 decade ascribed to climate change superimposed by biological processes

Clargo, Nicola M.; Salt, Lesley A.; Thomas, Helmuth; de Baar, Hein J. W.

Published in:
Marine Chemistry

DOI:
10.1016/j.marchem.2015.08.010

Publication date:
2015

Marine Chemistry 177 (2015) 566–581

Contents lists available at ScienceDirect

Marine Chemistry

journal homepage: www.elsevier.com/locate/marchem

Rapid increase of observed DIC and pCO_2 in the surface waters of the North Sea in the 2001-2011 decade ascribed to climate change superimposed by biological processes

Nicola M. Clargo [a,*], Lesley A. Salt [b], Helmuth Thomas [c], Hein J.W. de Baar [a]

[a] Royal Netherlands Institute for Sea Research, Landsdiep 4, 1797 SZ, Texel
[b] CNRS, UMR 7144, Equipe Chimie Marine, Station Biologique de Roscoff, Place Georges Teissier, 29680 Roscoff, France
[c] Department of Oceanography, Dalhousie University, Halifax, B3H 4R2, Nova Scotia, Canada

ARTICLE INFO

Article history:
Received 30 January 2015
Received in revised form 25 August 2015
Accepted 27 August 2015
Available online 4 September 2015

Keywords:
Carbon dioxide (CO_2)
Shelf Seas
Dissolved Inorganic Carbon
Air-sea CO_2 exchange
North Sea
Mechanisms of Ocean Acidification

ABSTRACT

The CO_2 system in the North Sea over the 2001-2011 decade was investigated using four comprehensive basin-wide datasets covering the late summer periods of 2001, 2005, 2008 and 2011. We find that rises in surface water DIC and pCO_2 exceeded concurrent rises in atmospheric pCO_2, which we attribute primarily to biological activity in late summer. After accounting for this biological signal, the observed ocean acidification occurs at a rate that is consistent with concurrent atmospheric and open ocean CO_2 increases over the 2001-2011 decade. Nevertheless, we do find a consistent reduction in CO_2 undersaturation in the NNS and an increase in CO_2 supersaturation in the SNS. We propose that the synergistic effects of increasing atmospheric pCO_2 and subsequent decrease in seawater buffering capacity, together with rising sea surface temperatures in the future oceans, may reduce the strength of the North Sea as a CO_2 sink. Such a reduction would diminish the efficiency of this region as a continental shelf pump with respect to uptake of CO_2 by the sea. Ultimately this would constitute a positive feedback mechanism, i.e. enhancing the airborne fraction of anthropogenic CO_2 and thus the net rate of increase of atmospheric pCO_2 and subsequent global climate change.

1. Introduction

The increase of atmospheric concentrations (partial pressures) of carbon dioxide (CO_2) as a result of anthropogenic activity is a well-documented phenomenon that not only affects global climate via the process known as "global warming", but also has implications for the chemistry of the global oceans. An estimated 29 % (170 ± 20 GtC) of the total anthropogenic emissions of CO_2 released to the atmosphere from 1750 – 2013 has been absorbed by the oceans, thus constituting a significant CO_2 sink (Le Quéré et al., 2014). Absorption of CO_2 across the air-sea interface is thermodynamically driven by the difference in partial pressure between seawater (pCO_{2sw}) and the overlying air: $\Delta pCO_2 = pCO_{2sw} - pCO_{2atm}$. In the absence of other processes, increasing pCO_{2atm} will drive a concurrent increase in pCO_{2sw}. The rise in atmospheric pCO_2 is currently occurring at a rate of 2.1 μatm yr^{-1} (http://co2now.org/). However, pCO_{2sw} and therefore ΔpCO_2 is regulated by additional physical processes in the ocean, such as variations in sea surface temperature (SST), the upwelling of CO_2-enriched deep water, and by biologically induced variations in the concentrations of dissolved inorganic carbon (DIC) and total alkalinity (A_T) (Takahashi et al., 2002). Throughout the euphotic zone, the opposing processes of primary production and remineralisation cause the uptake and release of DIC, respectively. Furthermore, calcification by marine organisms is another process influencing both DIC and A_T, although in a 1:2 ratio, as the production of $CaCO_3$ removes two moles of A_T and one mole of DIC for each mole of $CaCO_3$ produced.

Shelf seas have been shown to have greater seasonal ΔpCO_2 amplitudes than oceanic areas at the same latitude (Thomas and Schneider, 1999; Thomas et al., 2004). Due to their role as a link between terrestrial and oceanic systems, these regions are highly dynamic environments, subject to large variations in hydrographic properties such as temperature and salinity, as well as large inputs of organic matter and inorganic nutrients from terrestrial sources. As a result, shelf seas are highly productive, accounting for an estimated 10-30% of the primary productivity of the global oceans, whilst only covering 7% of their surface area, and therefore they play an important role in the global carbon cycle (Gattuso, et al., 1998). However they also show great heterogeneity (Chen and Borges, 2009).

Furthermore, some shelf seas have been identified as 'continental shelf pumps' with respect to carbon (Tsunogai et al., 1999), as has been shown for the North Sea (Thomas et al., 2004). Situated on the Northwestern European shelf, the North Sea can be divided into two biogeochemically-distinct regions: the Northern North Sea (NNS) and

* Corresponding author.
E-mail addresses: nikki.clargo@nioz.nl (N.M. Clargo), lesley.salt@sb-roscoff.fr (L.A. Salt), helmuth.thomas@posteo.org (H. Thomas), Hein.de.Baar@nioz.nl (H.J.W. de Baar).

http://dx.doi.org/10.1016/j.marchem.2015.08.010
0304-4203/

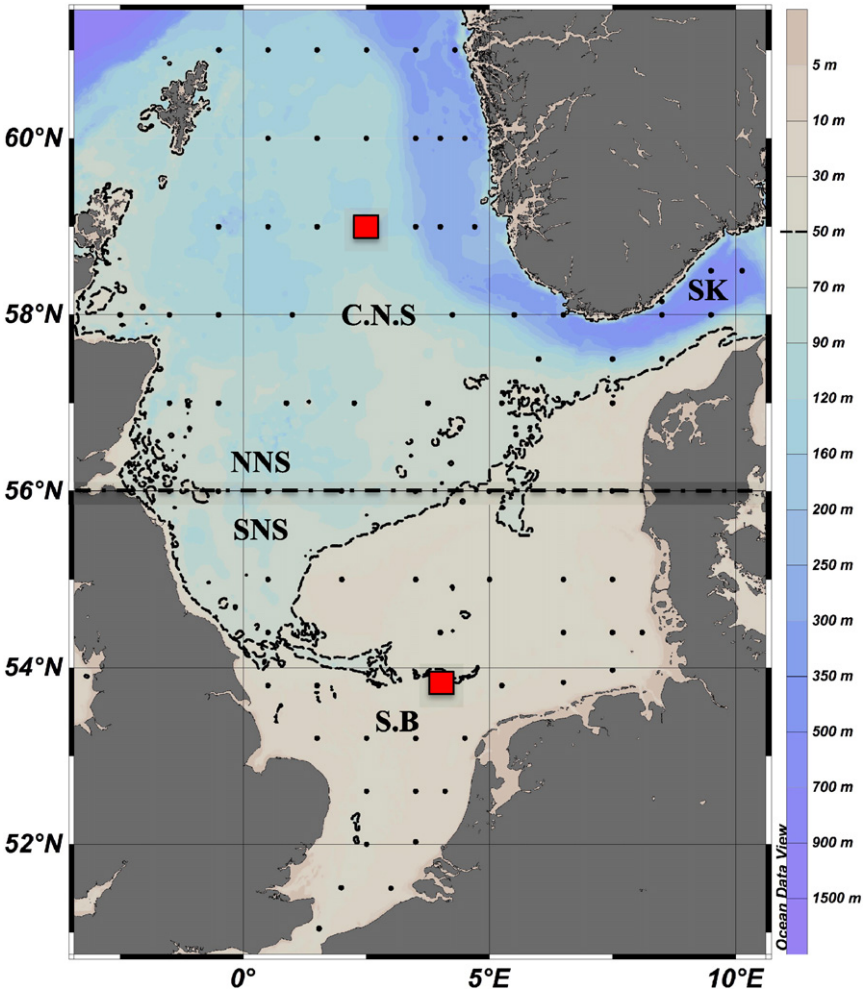

Fig. 1. Map of the North Sea basin, with the divide between the NNS and SNS along 56 °N highlighted by the dashed line and the representative stations for each region (59 °N, 2.5 °E for the NNS, and 53.8 °N, 4 °E for the SNS) highlighted by the red squares. The abbreviations indicate the locations of the Central North Sea (C.N.S), Southern Bight (S.B) and the Skagerrak (SK), and the black dots represent the original station locations, common to each of the four summer cruises. This plot was created using Ocean Data View (Schlitzer, R., Ocean Data View, http://odv.awi.de, 2015).

Southern North Sea (SNS) (Fig. 1) that are largely determined by the bathymetric divide of the 50 m depth contour. In the deeper waters of the NNS (~150 m on the shelf and ~700 m in the Norwegian Trench), seasonal stratification sets up a summertime boundary between the upper mixed layer and the water below the seasonal pycnocline. This causes the establishment of an autotrophic system in the surface waters, whereby primary production reduces ambient DIC concentrations. Upon settling of biogenic debris, its remineralisation in subsurface waters then yields release of metabolic DIC into these subsurface waters (Thomas et al., 2004; Wakelin et al., 2012). Stratification prevents this DIC from being mixed back into the surface layer, with two principle effects. Firstly the DIC removed from surface waters is replenished by pCO_{2atm} to counteract the undersaturation. This summertime drawdown in the NNS of atmospheric CO_2 constitutes approximately 2.4 - 3.8 mmol C m^{-2} d^{-1} (Bozec et al., 2005). Secondly, due to water mass circulation, the vast majority of the remineralised DIC within the subsurface waters is transported out into intermediate waters of the North Atlantic (Wakelin et al., 2012), without further contact with the atmosphere. This is a result of the dominant anti-clockwise circulation of the North Sea and a regional subsurface water residence time of the order of one year or less (Lenhart et al., 1995). It is this net transport of carbon from the atmosphere via surface coastal waters into deep oceanic waters that is termed the "continental shelf pump".

In contrast, the SNS is a shallow region where strong tidal mixing results in the absence of stratification and therefore a one-compartment water column. As a result, the processes of primary production and remineralisation are not spatially separated and the system is predominantly heterotrophic in the summer, whereby the remineralised carbon is released back into the single-layer water column. The subsequent reduction in the difference in partial pressure between the surface water and the overlying atmosphere leads to a smaller air/sea exchange (flux) of CO_2. In addition to the release of remineralised carbon, higher SST in the SNS, in comparison to the NNS, leads to the supersaturation of CO_2 in SNS waters, with subsequent outgassing of CO_2 to the overlying atmosphere. Thus this region acts as a summertime source of CO_2, with an estimated summertime efflux of 0.8 - 1.7 mmol m^{-2} d^{-1} from the sea to the atmosphere (Bozec et al., 2005).

The summertime dichotomy of pCO_2 in the surface waters of the NNS and SNS has been well documented (Thomas et al., 2004; Bozec et al., 2005; Prowe et al., 2009; Omar et al., 2010; Salt et al., 2013). Biological activity acts as the dominant driver of summertime pCO_2 fluxes in the NNS (Thomas et al., 2005a; Prowe et al., 2009), however, in the SNS there is some dispute as to whether temperature (Prowe et al., 2009, Kühn et al., 2010) or biological activity (Schiettecatte et al., 2007) is the dominant driver. Nevertheless, during the late summer period, the North Sea basin as a whole has been shown to constitute a weak sink of CO_2, with an estimated uptake of 1.5 to 2.2 mmol C m^{-2} d^{-1} (Bozec et al., 2005).

The continued flux of CO_2 from the atmosphere into the ocean causes an increase in bicarbonate ions (HCO_3^-), a decrease in carbonate

ions (CO_3^{2-}) and an increase in hydrogen ions (H^+). These changes lead to a decrease in pH that is commonly termed "Ocean acidification" in the literature, which is projected to continue as atmospheric pCO_2 continues to rise, with potentially deleterious effects at the individual, species, and ecosystem level (Doney et al., 2009). However, due to a paucity of long-term observational data in coastal regions, it has often been difficult to distinguish between considerable natural variability and long-term trends attributable to rising atmospheric CO_2, and therefore the development of reliable models for coastal seas is particularly important. Wakelin et al. (2012) found the Northeast Atlantic, including the European Shelf, to be a net sink for CO_2 in a simulation from 1989 – 2004, with biological activity acting as a stronger driver of air-sea CO_2 flux than temperature. Lorkowski et al. (2012) simulated changes in the North Sea CO_2 system from 1970 – 2006 and suggest that the principle drivers for variations in air-sea CO_2 flux are temperature, net ecosystem production and pH.

Furthermore, with continued invasion of atmospheric CO_2 into the oceans, the buffering capacity of surface waters is decreasing, whereby as the surface ocean absorbs more CO_2, its capacity for further uptake of CO_2 is reduced. This is indeed thought to be occurring in the North Sea, as shown by observational studies (Thomas et al., 2007) and as predicted by model simulations for this region (Lorkowski et al., 2012), who found that an increase in temperature combined with a decrease in pH led to a 30 % decrease in the CO_2 uptake capacity of the North Sea over the period of their simulation.

With the increasing availability of carbon system datasets spanning longer time periods, it is becoming possible to elucidate anthropogenically-induced trends based upon observational data, and to validate model predictions. A recent review of a suite of time-series studies covering 15-30 years of the carbon system in surface waters in various locations around the globe reporting acidification at rates that were concurrent with atmospheric CO_2 increases (Bates et al., 2014). However, several studies have indicated that certain shelf seas may be experiencing changes that are occurring faster than those that would be expected due to rising atmospheric pCO_2 (Thomas et al., 2007, Wootton et al., 2008). In order to determine whether or not this is the case for the North Sea, we present new data from a cruise in the late summer of 2011, and in combination with previous observational datasets, investigate here the carbon system of the North Sea over the 2001-2011 decade.

2. Materials and methods

2.1. Dataset

Four late summer cruises were undertaken aboard RV Pelagia on: 18/08 – 13/09/2001; 17/08 – 05/09/2005; 21/08 – 07/09/2008 and 01-25/09/2011. A 1° by 1° grid of approximately 90 stations was occupied during each cruise and sampled via a Conductivity Temperature Depth (CTD) system. This yielded the standard suite of oceanographic data, comprising temperature, salinity (derived from conductivity), pressure, and oxygen (Bozec et al., 2005, 2006; Thomas et al., 2007; Salt et al., 2013). Discrete samples were also collected for the measurement of the inorganic nutrients nitrate (NO_3), phosphate (PO_4) and silicate ($Si(OH)_4$).

The 2001-2008 data have been released as part of the EU-FP7 CARBOOCEAN activities. The 2011 data will be released in accordance with the rules imposed by the funding agency (NWO).

2.1.1. Measured parameters

2.1.1.1. DIC and A_T. Discrete water samples were collected at each station over the total depth range and analysed for dissolved inorganic carbon (DIC_{obs}) and alkalinity (A_T). All collection and analysis techniques were carried out as described in Dickson et al. (2007). Water samples were collected using borosilicate glass bottles and stored in the dark before being measured within 12 hours. Measurements were conducted through the use of VINDTA 3C's (Versatile INstrument for the Determination of Titration Alkalinity, Marianda, Kiel), which are capable of simultaneously analysing samples for DIC and A_T via coulometric and potentiometric titrations, respectively.

Quality control and calibration were achieved by the use of Certified Reference Material (CRM) from Prof. Andrew Dickson at Scripps Institute of Oceanography, San Diego, California. As we assume that our measurements of CRMs are 100% accurate, we can only calculate precision for DIC_{obs} and A_T data. We quote precision as the standard deviation of replicate samples, which for the 2011 data was $\pm$ 1 μmol kg^{-1} for A_T, based on 161 replicates, and $\pm$ 2 μmol kg^{-1} for $DIC_{obs,}$ based on 156 replicates. In comparison, for the 2001 and 2005 cruises, precision was calculated at $\pm$ 2-3 μmol kg^{-1} for A_T, and $\pm$ 1.5 μmol kg^{-1} for DIC_{obs} (Thomas et al., 2007). For 2008, precision was given as $\pm$ 1.6 μmol kg^{-1} for A_T and $\pm$ 2.1 μmol kg^{-1} for DIC_{obs}.

The 2011 cruise DIC_{obs} and A_T data have also been investigated by Burt et al. (2015).

2.1.1.2. Oxygen. Discrete oxygen samples were measured in duplicate following the Winkler titration method (Winkler, 1888). These were then collated with the CTD, nutrient and carbon data. Based upon replicate samples, precision of these data was calculated as $\pm$ 0.5 O_2 μmol l^{-1}).

2.1.1.3. Ancillary Parameters. The CTD system was mounted on a standard rosette frame, comprised of 24 x 25 l Ocean Test Equipment niskin bottles. The accuracy of each of the instruments on the CTD package is quoted by the manufacturer (Sea-Bird Electronics) as the following: conductivity to $\pm$ 0.003 S/m, temperature to $\pm$ 0.001 °C and pressure to $\pm$ 0.015% of full scale (http://www.seabird.com/sbe911plus-ctd, 2015). Salinity is derived from conductivity, and has been shown to be accurate to $\pm$ 0.0033 PSU (Le Menn, 2011).

Discrete samples were also collected for the determination of inorganic nutrients and were measured simultaneously using a QuAAtro Continuous Flow Analyser, with channels measuring silicate ($Si(OH)_4$), phosphate (PO_4), nitrite (NO_2), a combination (NOx) of nitrate (NO_3) and nitrite (NO_2), and ammonium (NH_4^+). Measurements were calibrated using low nutrient seawater (LNSW) at a salinity range similar to that found in the North Sea. Accuracy cannot be stated for these data but the analysis group performs well in global intercomparison studies. Precision was calculated using the standard deviation of duplicate samples between runs and is quoted as the following: $\pm$ 0.058 μmol l^{-1} Si for $Si(OH)_4$; $\pm$ 0.014 μmol l^{-1} P for PO_4; $\pm$ 0.017 μmol l^{-1} N for NO_2; $\pm$ 0.087 μmol l^{-1} N for NOx and $\pm$ 0.057 μmol l^{-1} N for NH_4^+ (NIOZ, S.Ossebaar, pers.comm).

2.2. Calculations

2.2.1. Data manipulation

Data collected during each of the cruises were consolidated and matched by location, to within 0.2° latitude, 0.2° longitude and 20 % of the depth. To ensure comparability only A_T or DIC_{obs} data available from the same station and depth for all four years were collated. This resulted in 81 comparable stations. These data were then gridded to a 0.5° resolution in order to prevent bias due to sampling density. Finally, due to differences in the number of data points between parameters, to ensure a fair comparison only gridded data that occurred at the same point in all four years were used for the analysis of each parameter.

For the purposes of this paper, the Northern North Sea and Southern North Sea shall be defined as >56 °N and <56 °N, respectively (Fig. 1), and henceforth be referred to as the NNS and SNS. This latitude has been selected as it represents the approximate position of the 50 m depth contour, which has been used previously to distinguish between the two regions (Salt et al., 2013, Queste et al., 2013). The surface refers to the upper 10 m of the water column.

2.2.2. Resolving the carbon system using CO2SYS

We used DIC_{obs} and A_T to calculate a suite of other carbon system parameters using the MATLAB version of CO2SYS (Lewis and Wallace, 1998, van Heuven et al., 2011). Additional input parameters were: temperature, salinity, pressure, $Si(OH)_4$, and PO_4, with the specified carbonic acid dissociation constants, K_1 and K_2, of Mehrbach et al. (1973) refitted by Dickson and Millero (1987). Calculated parameters include: partial pressure of CO_2 (pCO_2), pH, Revelle factor, HCO_3^-, CO_3^{2-}, $\Omega_{Calcite}$ and $\Omega_{Aragonite}$.

Calculation error (CE) was calculated through the use of CO2SYS. The precision of the DIC_{obs} and A_T measurements were applied to the dataset for each cruise, thereby establishing an upper and lower limit of Measurement Error (ME), yielding DIC_{max}, DIC_{min}, A_{Tmax} and A_{Tmin}. These were then used as input parameters for CO2SYS, in conjunction with the associated hydrographic and nutrient data, which have estimated errors that are smaller than those estimated for DIC_{obs} and A_T, and are thus accounted for here. The following combinations were run through CO2SYS: DIC_{max} with A_{Tmin} and DIC_{min} with A_{Tmax}, to obtain a set of carbonate parameters with the largest error margin possible. The minimum value for each parameter was then subtracted from the maximum value, and the CE (or mean difference) was divided by two to give an error margin on both sides of the calculated value.

2.2.3. Calculation of abiotic DIC (aDIC)

Abiotic DIC (aDIC) was calculated in order to remove the effects of primary productivity and respiration on DIC_{obs}, thereby removing the effects of differences in these biological processes between years. Firstly, Apparent Oxygen Utilisation (AOU) was calculated (Eq. (1)). This term describes the biological activity experienced by a parcel of water since it was last at equilibrium with the O_2 concentration of the atmosphere, and was calculated using the equilibrium saturation (as a function of salinity and temperature) of O_2 with the atmosphere (O_{2sat}) and the discrete oxygen data (O_{2meas}):

$$AOU = [O_2]_{sat} - [O_2]_{meas} \quad (1)$$

This was then used to calculate aDIC, using DIC_{obs} and the application of the factor 0.7 representing the Redfield ratio (Anderson and Sarmiento, 1994), which is comparable with a mean coefficient of 0.8 that we obtain in our calculation of DIC_{base} (see Section 2.2.6):

$$aDIC = DIC_{obs} - (AOU * 0.7) \quad (2)$$

Here the term (AOU*0.7) represents the portion of DIC gain or loss due to net respiration or net photosynthesis, respectively. The balance of these processes is termed Net Ecosystem Production (NEP): NEP = NPP – HR, where NPP is net primary production and HR is heterotrophic respiration. Thus, positive NEP occurs when NPP > HR; the system is described as being net autotrophic and acts as a net sink for atmospheric CO_2. Conversely, negative NEP indicates that NPP < HR, therefore the system is net heterotrophic and constitutes a net source of CO_2 to the atmosphere.

2.2.4. Calculation of DIC_{bio}

An alternative approach to approximate the DIC gain or loss due to biological effects is by the derivation of the term DIC_{bio} (Borges, 2011; Burt et al., 2015), which will account for changes due to primary production and respiration, as well as the biological formation of calcium carbonate (CaCO3) and/or its dissolution. Briefly, primary production and its reverse i.e. respiration, affect the DIC, whereas biocalcification/dissolution affects both DIC and A_T. We inherently consider any biological impact on A_T via the inclusion of in-situ data in our calculation of DIC_{bio}, which was entered as an input parameter into the MATLAB version of CO2SYS, in addition to in-situ temperature, salinity and nutrient data. We then calculated the DIC concentrations that would be observed assuming that the seawater would be at equilibrium with the atmospheric CO_2 partial pressure, i.e. $pCO_{2atm} = pCO_{2sw}$ then yields DIC_{atm}. The differences between this calculated DIC_{atm} and DIC_{obs} (DIC_{bio}, Eq. (3)) thus indicate the presence and extent of additional biological sources or sinks of DIC in the North Sea, under the assumptions that the surface waters are equilibrated with respect to atmospheric CO_2 prior to the onset of biological activity, and that CO_2 air-sea exchange is slow or negligible at a shorter time scale. A further underlying assumption is that surface water temperature does not vary, or varies only incrementally at the time scale applicable to DIC_{bio}. The relevant integration time scale is sub-seasonal (approximately several weeks). Given the timing of our cruises at the end of the summer period, the temperature had been relatively stable at the summer plateau (see for example Prowe et al., 2009), or had just started to slowly decrease. We argue that the effect of temporal variability in temperature is minor here, and if present, the decrease in temperature would yield an underestimation of the respiratory i.e. positive component of DIC_{bio}.

The input pCO_{2atm} used for the calculation was the monthly averaged atmospheric CO_2 partial pressure for the time period that corresponded to each cruise, using data collected at the Mace Head Atmospheric Research Station, Ireland (National Oceanographic and Atmospheric Association at their website: ftp://aftp.cmdl.noaa.gov/data/trace_gases/co2/flask/surface/co2_mhd_surface flask_1_ccgg_month.txt). In order to calculate errors for DIC_{atm}, we followed the same procedure as detailed in Section 2.2.2, using a combination of atmospheric pCO_2 partial pressures from Mace Head, supplied with an estimated measurement error of ±0.09 ppm (Earth System Research Laboratory, National Oceanic and Atmospheric Administration, Ed Dlugokencky pers.comm), and measured A_T.

DIC_{bio} was then calculated using the following equation:

$$DIC_{bio} = DIC_{obs} - DIC_{atm} \quad (3)$$

This term provides an alternative means of inferring biological activity, via the removal of the impact of hydrographic variability on DIC_{obs}.

2.2.5. Comparison of aDIC and DIC_{bio}

In order to assess the validity of our calculations outlined in Sections 2.2.4 and 2.2.5, we compare the two biological DIC approximations, DIC_{bio} with (DIC_{obs} – aDIC) for each location. It should be stated that these two different methods are applicable to different sections of the water column. The underlying assumption in the calculation of DIC_{bio} is that equilibrium exists between the water and the atmosphere, and that other processes are not altering DIC, thus this is only applicable to surface waters. In contrast, due to the rapid equilibrium between the surface waters and the overlying atmosphere with respect to oxygen, AOU is not necessarily representative of net biological activity in surface waters, but better reflects biological processes (i.e. respiration) in subsurface water. Furthermore, (DIC_{obs}- aDIC) does not account individually for the biological effects of $CaCO_3$ formation and dissolution, whereas these effects are inherent in our calculation of DIC_{bio}. We therefore expect that differences between the two methods will be at least partly due to this.

For the un-gridded water column data the mean difference (DIC_{bio} – (DIC_{obs} - aDIC)) between the two methods is consistently close to 0 (-2.5 to -0.1μmol kg^{-1}) and shows a normal distribution with standard deviations of: 25 μmol kg^{-1}; 16 μmol kg^{-1}; 16.3 μmol kg^{-1}; and 21.1μmol kg^{-1}, for 2001, 2005, 2008 and 2011, respectively. For the gridded surface data, the mean and standard deviation of the difference between the two methods was: -10.9 μmol kg^{-1} and 32.6 μmol kg^{-1}; -2.9 μmol kg^{-1} and 16.9 μmol kg^{-1}; -0.26 μmol kg^{-1} and 18.1 μmol kg^{-1}; and -0.4 μmol kg^{-1} and 21 μmol kg^{-1} for 2001, 2005, 2008 and 2011, respectively.

We suggest that the standard deviation of the differences between DIC_{bio} and (DIC_{obs}-aDIC) are less than, or comparable to, the uncertainty given for DIC_{bio} in Table 1. Therefore, for the purpose of this study, we consider both methods valid.

Table 1
Mean and standard deviation of gridded surface (< 10 m) oceanographic and carbon system data from all four summer cruises. Numbers in italics indicate the number of data points. Atmospheric pCO_2 concentrations supplied by Mace Head National Oceanographic and Atmospheric Association at their website (ftp://aftp.cmdl.noaa.gov/data/trace_gases/co2/flask/surface/co2_mhd_surface-flask_1_ccgg_month.txt, 2015).

Year	Temperature (°C)	Salinity	AOU (μmol kg^{-1})	DIC (μmol kg^{-1})	AT (μmol kg^{-1})	*p*CO2 (μatm)	Atmospheric *p*CO2 (μatm)	ΔpCO_2 (μatm)	$npCO_2$ (μatm)	$\Delta npCO_2$ (μatm)	DIC_{BIO} (μmol kg^{-1})
Basin-wide											
2001	15.7 ± 1.5	34.19 ± 0.97	-17.2 ± 9.1	2033 ± 39	2294 ± 28	328 ± 63	361.88 ± 0.09	-33.4 ± 62.7	327 ± 54	-34.5 ± 53.6	-23.46 ± 37.15
	290	*290*	*282*	*284*	*290*	*262*		*262*	*262*	*262*	*262*
2005	14.92 ± 1.37	34.24 ± 1.05	-12.8 ± 5	2058 ± 27	2299 ± 28	354 ± 35	373.22 ± 0.09	-18.7 ± 34.5	367 ± 29	-6.1 ± 28.6	-10.56 ± 17.48
	290	*290*	*282*	*284*	*290*	*262*		*262*	*262*	*262*	*262*
2008	15.84 ± 1.09	34.13 ± 1.15	-10.3 ± 3.9	2056 ± 34	2294 ± 33	369 ± 39	377.68 ± 0.09	-8.5 ± 38.6	370 ± 30	-7.3 ± 30.4	-5.34 ± 19.1
	290	*290*	*282*	*284*	*290*	*262*		*262*	*262*	*262*	*262*
2011	14.24 ± 1.55	34.16 ± 1.09	-3.3 ± 4.4	*2074 ± 29*	2293 ± 30	385 ± 43	383.36 ± 0.09	1.8 ± 42.7	411 ± 30	27.5 ± 29.5	-0.45 ± 19.27
	290	*290*	*282*	*284*	*290*	*262*		*262*	*262*	*262*	*262*
NNS (>56 °N)											
2001	14.87 ± 1.19	34.29 ± 1.02	-20.3 ± 9.6	2009 ± 28	2286 ± 25.69	281 ± 31	_	-81 ± 31.2	290 ± 27	-71.7 ± 27.1	-51.35 ± 23.77
	164	*164*	*156*	*158*	*164*	*136*		*136*	*136*	*136*	*136*
2005	14.16 ± 1.16	34.13 ± 1.2	-12.6 ± 4.29	2044 ± 26	2290 ± 30.02	333 ± 14	_	-40.6 ± 13.7	356 ± 14	-17.5 ± 13.7	-21.45 ± 7.59
	164	*164*	*156*	*158*	*164*	*136*		*136*	*136*	*136*	*136*
2008	15.42 ± 0.92	33.90 ± 1.42	-11.5 ± 3.44	2039 ± 31	2285 ± 35.25	342 ± 20	_	-36.1 ± 19.8	350 ± 20	-27.5 ± 20.1	-18.97 ± 10.26
	164	*164*	*156*	*158*	*164*	*136*		*136*	*136*	*136*	*136*
2011	13.30 ± 0.84	33.99 ± 1.28	-2.7 ± 4.84	2061 ± 29	2282 ± 33.88	356 ± 24	_	-27.8 ± 24.1	397 ± 26	13.4 ± 26.4	-14.15 ± 11.93
	164	*164*	*156*	*158*	*164*	*136*		*136*	*136*	*136*	*136*
SNS (<56 °N)											
2001	16.78 ± 1.12	34.06 ± 0.88	-13.4 ± 6.7	2063 ± 29	2306 ± 28	380 ± 45	_	18 ± 45	368 ± 46	5.7 ± 45.6	6.64 ± 22.63
	126	*126*	*126*	*126*	*126*	*126*		*126*	*126*	*126*	*126*
2005	15.91 ± 0.94	34.37 ± 0.79	-13.1 ± 5.8	2074 ± 17	2310 ± 19	378 ± 35	_	4.9 ± 34.7	379 ± 35	6.2 ± 34.7	1.18 ± 17.54
	126	*126*	*126*	*126*	*126*	*126*		126	*126*	*126*	*126*
2008	16.38 ± 1.06	34.44 ± 0.51	-8.8 ± 4	2077 ± 25	2306 ± 25	399 ± 31	_	21.2 ± 31.3	392 ± 24	14.5 ± 23.8	9.37 ± 15.1
	126	*126*	*126*	*126*	*126*	*126*		*126*	*126*	*126*	*126*
2011	15.46 ± 1.39	34.38 ± 0.73	-4.1 ± 3.7	2091 ± 19	2307 ± 16	417 ± 35	_	33.7 ± 34.6	426 ± 25	42.6 ± 24.9	14.34 ± 14.05
	126	*126*	*126*	*126*	*126*	*126*		*126*	*126*	*126*	*126*

2.2.6. Calculation of DIC_{base}

As during this time of year production and remineralisation are consistently ongoing, for this study, direct comparisons of DIC values are problematic. Below the surface layer, the covariance of AOU and DIC_{obs} is used to infer a "baseline" DIC, which is the theoretical DIC that the parcel of water would have if no primary production or respiration was taking place. We calculate this for each station by plotting subsurface DIC_{obs} against AOU (AOU on x-axis, DIC_{obs} on y-axis (for examples stations, see Fig. 2), such that remineralisation is indicated by positive AOU, and primary production inferred by negative AOU. The points for each station are regressed using a robust regression, and the point at which this line crosses the y-axis, that is when AOU = 0, is taken as the "baseline" DIC value, hereon throughout referred to as DIC_{base}.

The shallow nature of the SNS and certain hydrographic features in the NNS (such as the Norwegian Trench) caused significantly greater residuals in the model, for affected stations. For this reason, we selected stations with residuals < 10, which accounted for on average 78 ± 1 % of stations for all four years. The mean slope yielded using every regression for our selected stations is 0.8, which is close to the factor of 0.7 used to calculate aDIC (see Eq. (2)). We then gridded these data across the North Sea basin, as described in Section 2.2.1, and finally calculated mean values for the NNS and SNS. In order to estimate errors for DIC_{base}

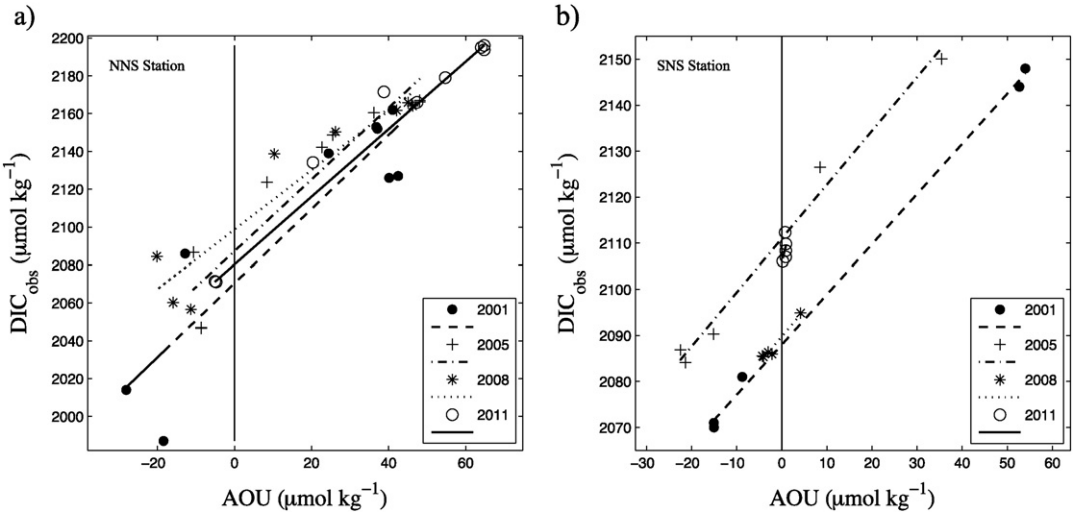

Fig. 2. DIC_{base} plots for a) NNS station (59 °N, 2.5 °E) and b) SNS station (53.8 °N, 4 °E). Lines represent the robust fit of the data and symbols represent the data points. Please note, these stations are used as examples of the method of calculation and do not represent mean values for DIC_{base} in each region.

we quote the average one standard deviation of the residuals of each fit for each year, which result in error estimates of ± 4 μmol kg^{-1} ± 3.1 μmol kg^{-1} ± 2.8 μmol kg^{-1} and ± 3 μmol kg^{-1} for 2001, 2005, 2008 and 2011, respectively

2.2.7. Temperature-normalised pCO_2

To remove the effect of differences in sea surface temperature between cruises, pCO_2 data were normalised to a temperature of 16 °C ($npCO_2$). The temperature correction follows the equation of Takahashi et al. (2002):

$$npCO_2 = pCO_2 * \exp(0.0423. * (16 - \text{observed temperature})) \quad (4)$$

2.2.8. pCO_2 fluxes

We calculated the air-sea CO_2 flux, henceforth to be referred to as average CO_2 flux, following the method outlined in Takahashi et al. (2002), using:

$$F = k * \alpha * (\Delta pCO_2) \quad (5)$$

where k is the CO_2 gas transfer velocity, α is the solubility of CO_2 in seawater and ΔpCO_2 is the difference in pCO_2 between the surface ocean and atmosphere. To calculate k we used the gas transfer velocity of Nightingale et al. (2000), which actually was established in the North Sea, and average monthly wind speed data corrected to 10 m height, obtained from the NCEP/NCAR re-analysis project (Kalnay et al., 1996), and provided by the NOAA-ESRL Physical Sciences Division (Boulder, CO, USA, from their Web site at http://www.esrl.noaa.gov/psd/). We chose to use monthly averaged wind speed data, as opposed to data of a higher frequency, to reduce the influence of high wind events on our flux calculations, and therefore to better ensure that they represent conditions typical to the late summer season. Also, if we compare wind speeds of a higher resolution, our fluxes at different locations may be affected by different wind speeds, and the time period of one month corresponds to our observational window.

In contrast to previous investigations of pCO_2 in the North Sea, and for reasons of clarity and coherence, we here use the pCO_2 values that have been computed using DIC_{obs} and A_T, thus using a comparable method to our calculation of DIC_{bio} (Eq. (3)). While this might imply a computational uncertainty, the main purpose of the present study is to deepen our mechanistic understanding rather than to provide a highly resolved CO_2 air-sea flux budget. These data have a calculation error of ± 13 μatm, which was used to calculate maximum and minimum pCO_2 fluxes, the difference between which is represented by our error estimate.

We calculated the average CO_2 flux for the entire North Sea basin, and separately for the NNS and SNS, to elucidate trends over the 2001-2011 decade and to determine whether or not each region acted as a summertime source or sink of CO_2 for the atmosphere. To enable a comparison of the effects of temperature, biological activity and wind speed on the average CO_2 flux between years (although not necessarily with each other), we repeated the above flux calculation, substituting:

(i). pCO_2 for temperature-normalised pCO_2 to calculate $\Delta npCO_2$ (see Section 2.2.6), thereby normalizing the air-sea CO_2 flux to a temperature of 16 °C. We also altered k to account for this. We then calculated the normalised temperature anomaly by averaging the $npCO_2$ flux for all years, then subtracting each individual year from this average in order to compare the magnitude of the effect of temperature between years.

(ii). monthly-averaged wind speed for each cruise for the average monthly wind speed for all cruises, thus normalizing the air-sea CO_2 flux to a wind speed of 6.67 m/s. As with the temperature component, we then calculated a normalised wind anomaly (averaging wind-induced flux for all years and subtracting each individual year from this average value) to enable a comparison of the wind component between years.

(iii). pCO_2 for $pCO_{2abiotic}$. We first calculated pCO_2 using CO2SYS and A_T and aDIC as input parameters (see Section 2.2.3) and used this to calculate air-sea CO_2 flux. As this step effectively normalises the effect of biological activity to 0, subtracting this 'abiotic' flux from the average CO_2 flux yields a 'biological flux' that can be compared between years.

This method assumes superposition and linearity, as described in Pätsch and Lorkowski (2013), whereby we assume that we incorporate all processes affecting pCO_2. We account for changes to CO_2 solubility via the inclusion of in-situ temperature and salinity data as input parameters for CO2SYS. Similarly, we account for changes in A_T by including our in-situ A_T data. We therefore assume that only physical processes are left; namely advection and air-sea flux. Previous studies have divided the North Sea into 15 boxes and have shown that the residence time of these is of the order of one month (ICES, 1983). Given that our cruises were completed within less than this time period, we assume that advection is negligible. Therefore the only process remaining is air-sea flux.

3. Results

3.1. Observations

The basin-wide average gridded surface data of the principal hydrographic and carbonate parameters are summarised in Table 1, with averages also given for the SNS and NNS. Mean basin-wide surface temperatures were highest in the summers of 2001 (15.7 °C) and 2008 (15.84 °C) with the coldest being 2011 (14.24 °C), thus showing a total variation of 1.6 °C between years. The observed fall in temperature in 2011 was primarily driven by much colder surface temperatures in the NNS (13.3 °C), which were more than 2 °C colder than the SNS (15.46 °C). The disparity in temperature between the two regions can be observed throughout the 2001-2011 decade, with consistently warmer surface temperatures detected in the SNS, however, the gradient between the SNS and NNS varies between years. The distribution of salinity (not shown), on the other hand, is relatively uniform across the central North Sea basin, with the exception of lower salinities observed in regions that are in close proximity to fluvial influences and the Baltic outflow. The total range of mean salinity between years was 0.39 in the NNS, and 0.38 in the SNS, although no trends are evident within either of the two regions.

The basin-wide surface DIC_{obs} data for each of the four summer cruises are shown in Fig. 3. In 2001 and 2008, and to a lesser extent in 2005, a distinct boundary between the NNS and SNS that roughly correlates with the 50 m depth contour is evident. In comparison to the SNS, DIC_{obs} in the NNS is lower, with mean concentrations of 2009, 2044, 2039, and 2061 μmol kg^{-1} in 2001, 2005, 2008 and 2011, respectively. The regional minima are consistently found in the Skagerrak and close to the Norwegian coastline for all years, with a minimum observed in 2001 (1927 μmol kg^{-1}) and a maximum in 2011 (1974 μmol kg^{-1}). Particularly high concentrations (~2130 μmol kg^{-1}) are evident close to the Dutch, German and Danish coastlines, and are the result of fluxes of metabolic DIC out of the bordering Wadden Sea (Schwichtenberg, 2013, Burt et al., 2015), out of shallow sediments, and to a lesser extent, due to high concentrations within fluvial sources, given the location of the Elbe, Rhine and Scheldt estuaries in this region. These sources contribute to the higher DIC_{obs} values in the SNS for all four years; where mean concentrations were 2063, 2074, 2077 and 2091 μmol kg^{-1} in 2001, 2005, 2008 and 2011, respectively. As such, there is a minimum difference of 30 μmol kg^{-1} (max difference of 54 μmol kg^{-1}) between the SNS and NNS for all years, showing a significant DIC_{obs} gradient across the surface waters of the North Sea.

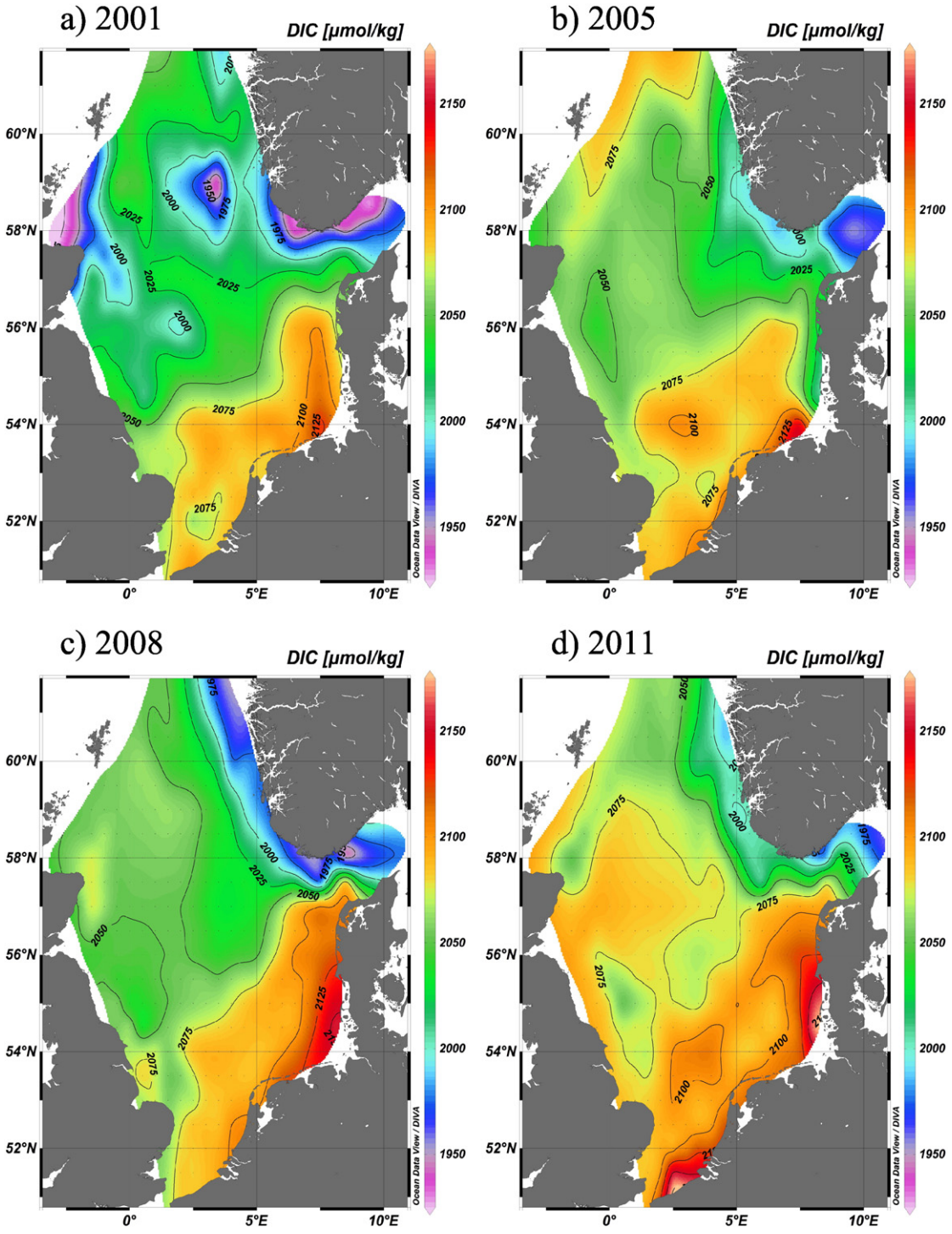

Fig. 3. Basin-wide surface layer distribution of gridded DIC data for the summers of: a) 2001; b) 2005; c) 2008 and d) 2011. This plot was created using Ocean Data View (Schlitzer, R., Ocean Data View, http://odv.awi.de, 2015), using DIVA gridding with an automatic scale length: X-scale-length [permille]= 21; Y scale-length [permille].

In the summers of 2005 and 2011, the boundary between the two regions is less apparent, with a difference in DIC_{obs} of 30 µmol kg^{-1} between the NNS and SNS found in both years. The lower north-south gradient is driven principally by higher DIC_{obs} values in the NNS, rather than by lower DIC values in the SNS. Minimum DIC_{obs} concentrations within the Baltic outflow are also not as extreme during 2005 and 2011: 1955 µmol kg^{-1} in 2005 and 1974 µmol kg^{-1} in 2011. Low concentrations of DIC_{obs} are evident along the Danish and German coastlines in the summer of 2005, which may be attributable to an increase in the southerly extent of the Baltic influence, or to high levels of primary production, as indicated by low DIC_{bio} (Fig. 4). Despite these regional changes, throughout the 2001-2011 decade mean basin-wide surface DIC_{obs} increased in both regions of the North Sea; by 52 µmol kg^{-1} in the NNS and by 28 µmol kg^{-1} in the SNS (Table 1). These increases led to a basin-wide DIC_{obs} increase of 41 µmol kg^{-1} in surface waters from 2001 to 2011.

In contrast to these variations in DIC_{obs}, variations in mean surface A_T (Table 1) over the 2001-2011 decade were small, with a range of only 8 µmol kg^{-1} in the NNS and 4 µmol kg^{-1} in the SNS. The A_T distribution (not shown here, see e.g. Burt et al., 2015) also remains stable between years,

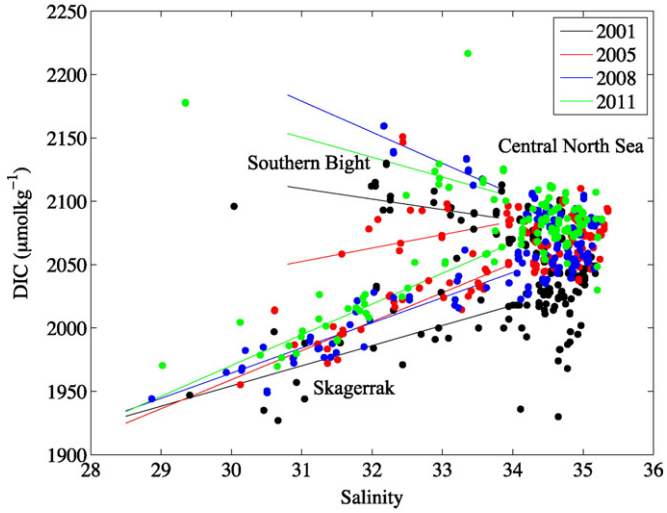

Fig. 4. Plot of surface water salinity versus DIC for the entire North Sea basin from all four summer cruises. Robust regression fits have the following equations for the Skagerrak region: DIC2001 = 15.9S + 1477; DIC2005 = 22.9S + 1273; DIC2008 = 19.9S + 1369; DIC2011 = 24.3S + 1243, and for the Southern Bight region: DIC2001 = -8.3S + 2367; DIC2005 = 10.6S + 1725; DIC2008 = -24.5S + 2938; DIC2011 = -15.6S + 2635.

and as with the similarly constant salinity, no temporal trend appears discernable. As a result of this stability, the calculated variations in pCO_2 are predominantly DIC-driven, with the additional impact of changes to hydrographic properties.

Mean surface water calculated pCO_2 increased substantially in both regions of the North Sea from 2001 to 2011: by 75 µatm in the NNS and 37 µatm in the SNS. These increases are appreciably larger than the observed increase of 21.48 µatm in atmospheric pCO_2 over the same time period. The imbalance in increases between the atmospheric and surface layer pCO_2 is indicative of the presence of processes other than those with a purely thermodynamic impact, driving the CO_2 system in seawater. Here we will focus our investigation on the drivers of the increasing DIC_{obs}, and thus pCO_2, in the North Sea over the 2001-2011 decade.

3.2. DIC vs. salinity

A mixing analysis indicates the presence of three water masses that constitute the North Sea (Fig. 4). These are the North Atlantic, Southern Bight, and Skagerrak, and the mixture of all three is known as Central North Sea water (Kempe and Pegler, 1991; Bozec et al., 2005). The Central North Sea water has a relatively high salinity (>34) as a result of the dominant influence of the North Atlantic water mass. In contrast, due to high fluvial input, the Southern Bight region has a characteristically lower salinity (32-34) but higher DIC concentrations (2100 - 2150 µmol kg^{-1}) and the Skagerrak region also has a low salinity due to the Baltic inflow, but markedly lower DIC concentrations (~ 1975 µmol kg^{-1}).

The aforementioned increase of DIC_{obs} in surface waters over the decade is also evident in Fig. 4, particularly within the Central North Sea water mass. Robust regression fits are applied to the Southern Bight – Central North Sea mixing line (data points chosen by salinity values and location) and the Skagerrak – Central North Sea mixing line, with considerable variability in the Southern Bight. Using the calculated regression fits for each year (shown in Fig. 4) for the Skagerrak - Central North Sea, we are able to determine a theoretical DIC at a salinity of 35, typical of the Central North Sea Water: 2034 µmol kg^{-1} for 2001; 2075 µmol kg^{-1} for 2005; 2066 µmol kg^{-1} for 2008 and 2094 µmol kg^{-1} for 2011. The theoretical DIC within this water mass increased steadily between 2001 and 2011, with the exception of a small decrease from 2005 to 2008, and therefore compares well with mean DIC_{obs}, as previously noted in the NNS (Table 1).

3.3. DIC_{bio}

3.3.1. Basin-wide DIC_{bio} distribution

Basin-wide surface plots of DIC_{bio} (see calculations Section 2.2.4) are shown in Fig. 5. In 2001, a clear division between the two biogeochemically distinct regions is immediately apparent, with net autotrophy indicated by negative DIC_{bio} values and hence biological uptake of DIC in the NNS, accounting for a mean of -51 µmol kg^{-1} of DIC. Positive DIC_{bio} (mean value of the four years = +8 µmol kg^{-1}) in the SNS indicates net heterotrophy in this region (see Burt et al., 2015 for details), leading to the production of excess DIC to that which would be present purely due to air-sea exchange of CO_2. DIC_{bio} is highly variable in the SNS, with a reduction from 7 µmol kg^{-1} to 1 µmol kg^{-1} between 2001 and 2005, and subsequent increases to 9 µmol kg^{-1} in 2008 and 14 µmol kg^{-1} in 2011. In contrast, over the decade, DIC_{bio} steadily becomes less negative in the NNS from a minimum of -51 µmol kg^{-1} in 2001 to -14 µmol kg^{-1} in 2011, representing a reduction in ongoing NEP at the time of sampling, although it should be noted that this may be the result of bias due to seasonal variability and changes in our observation window due to cruise timings.

The maximum values of DIC_{bio} are found along the coastlines of the UK and continental Europe, particularly in 2001 (47 µmol kg^{-1} off the coast of East Anglia) and in 2011 (65 µmol kg^{-1} at a station located off the German coast and in relatively close proximity to the Elbe outflow, see also Burt et al., 2015). The most negative values of -135 µmol kg^{-1} evident along the Scottish Coast and -115 µmol kg^{-1} on the Shetland Shelf in 2001 correspond with the particularly low mean surface DIC_{obs} concentrations shown in Fig. 3. Particularly high oxygen concentrations (355 µmol l^{-1}) were also observed at the same location close to the Scottish Coast, providing further evidence to support primary productivity as the cause of low DIC_{obs} concentrations.

3.4. Station Profiles

To further examine the effect of biological activity on DIC_{obs} in the two contrasting regions of the North Sea, we investigated the full water column at two selected stations: at 59°N, 2.5°E and at 53.8°N, 4°E (Fig. 1), representative of the NNS and SNS, respectively.

In the NNS, the vertical profiles (Fig. 6(a)) for all years clearly show the presence of stratification, with surface depletion of DIC_{obs}. The accompanying profile of AOU (Fig. 6(b)) indicates that in the surface layer the decrease in DIC_{obs} is due to primary productivity (indicated by negative AOU values), and sub-surface remineralisation of sinking organic matter below the mixed layer leads to much higher DIC_{obs} concentrations at depth. These profiles are also in agreement with the mean data for this region (Table 1), with DIC_{obs} at a minimum in 2001, with similar profiles apparent in 2005 and 2008, and with maximum DIC_{obs} throughout the water column in 2011.

With the exception of 2005, where stratification is evident, the AOU and DIC_{obs} vertical profiles in the SNS (Fig. 6(c)) are rather uniform with depth. Mixing of the relatively shallow water column in this region prevented stratification in 2001, 2008 and 2011, and therefore no physical boundary existed between the opposing processes of primary production and respiration. Contrary to the NNS, the range of values over the water column is much smaller, with the highest DIC_{obs} observed at depth in the summer of 2005. These profiles are in agreement with the regional average mean surface DIC_{obs} (Table 1), with minimum and maximum surface values observed in 2001 and 2011, respectively, and a higher DIC_{obs} in 2005 than observed in 2008.

It should be noted that AOU is not an appropriate measure of biological activity at the very surface (see Section 2.2.3), as by definition it is a measure of the change in the oxygen content of a water parcel since it was last at equilibrium with the atmosphere. Despite the fact that air-

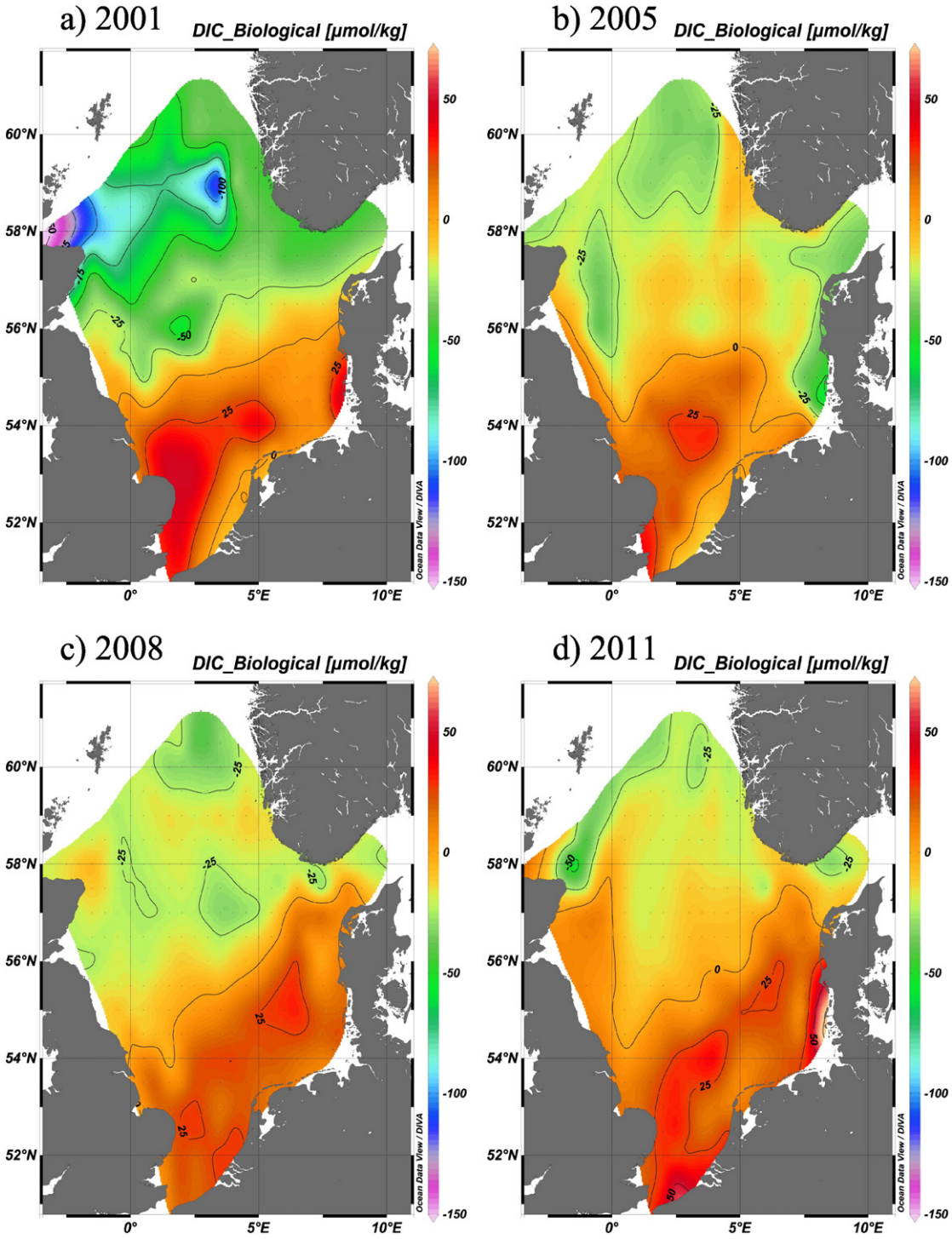

Fig. 5. Basin-wide surface layer distribution of gridded DIC_{bio} data (DIC_{obs}-DIC_{atm}) for the summers of: a) 2001 b) 2005 c) 2008 and d) 2011. This plot was created using Ocean Data View (Schlitzer, R., Ocean Data View, http://odv.awi.de, 2015), using DIVA gridding with an automatic scale length: X-scale-length [permille]= 22; Y scale-length [permille].

sea gas exchange of O_2 occurs very rapidly, the AOU profiles in Fig. 6 clearly indicate primary productivity above the mixed layer (i.e. negative values of AOU). Remineralisation is observed below it in the subsurface layers (i.e. positive AOU values), for all years at the NNS station, and for 2005 at the SNS station. Furthermore, the AOU profiles in the NNS show an apparent increase throughout the decade, which may be indicative of a reduction in primary productivity. This is also indicated by the aforementioned less negative values in mean surface DIC_{bio} (Table 1 and Fig. 5) and AOU in this region (Table 1). Further effects yielding these observations may be the effects of interannual variability combined with changes in the timing of our observations. In order to assess whether this trend is reflected in sub-surface waters, we integrated the AOU beneath the mixed layer depth in the NNS station, and by averaging over the applicable water depth, we calculate a deep station specific AOU of 40, 39, 42 and 60 mmol m^{-3} for 2001, 2005, 2008 and 2011, respectively.

At the SNS station, primary production was the dominant process throughout the water column for all years, with the exception of 2005, where AOU values below a depth of 20 m indicate that respiration prevailed.

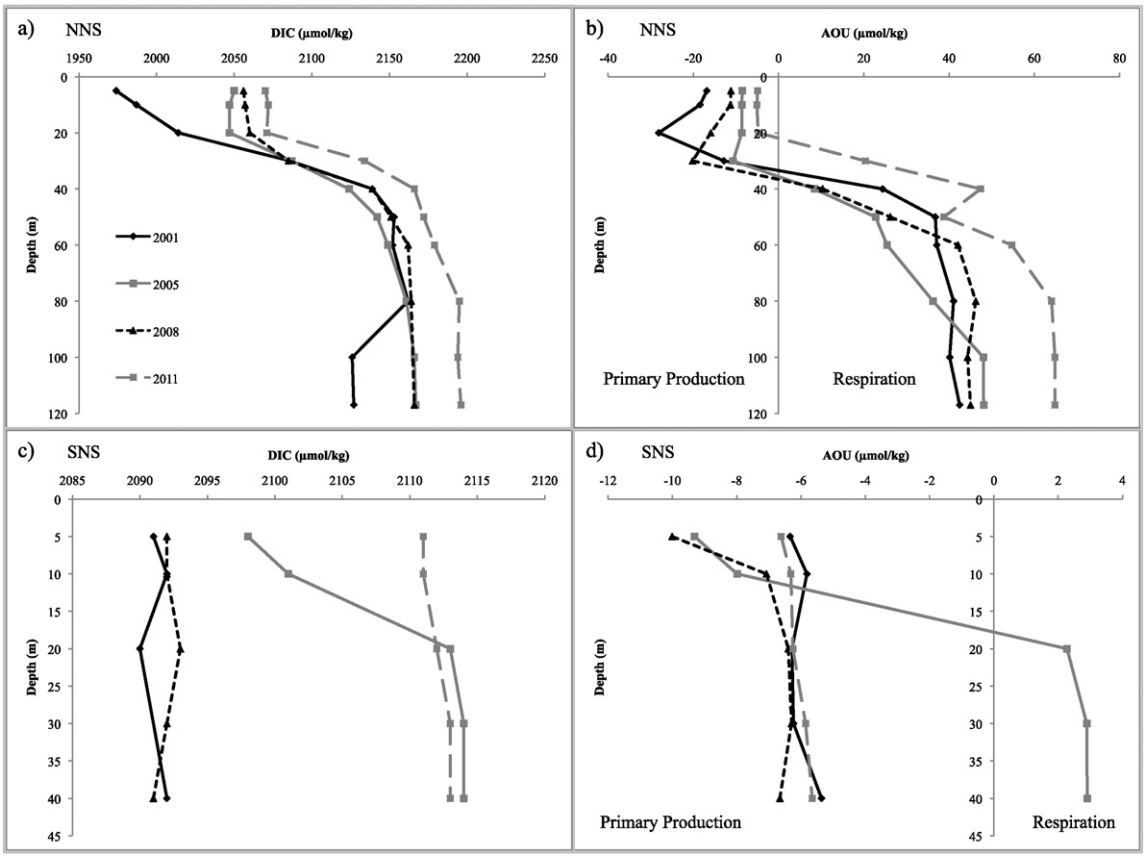

Fig. 6. Full-depth profiles of: a) NNS DIC b) NNS AOU c) SNS DIC and d) SNS AOU for all four summers. Representative stations are situated at 59 °N, 2.5 °E for the NNS, and 53.8 °N, 4 °E for the SNS.

3.5. DIC_{base}

Following the observed relationship between DIC_{obs} and AOU in both the SNS and NNS, we further used this relationship to estimate a background DIC value, or DIC_{base}, present in the North Sea (see methods Section 2.2.6). The results show that DIC_{base} was relatively stable in the SNS, with values of 2084 ± 4 µmol kg^{-1}, 2089 ± 3.1 µmol kg^{-1}, 2091 ± 2.8 µmol kg^{-1} and 2093 ± 3 µmol kg^{-1} for 2001, 2005, 2008 and 2011, respectively. There is somewhat greater variation in the NNS, with values of 2095 ± 4 µmol kg^{-1}, 2105 ± 3.1 µmol kg^{-1}, 2103 ± 2.8 µmol kg^{-1} and 2083 ± 3 µmol kg^{-1}, respectively. The relationship between AOU/DIC_{obs} shows significant positive correlations in the SNS, whereas the inverse relationship is apparent in the NNS, again showing the contrast in ongoing processes.

3.6. pCO2

In 2001, mean surface pCO_2 and ΔpCO_2 ($pCO_{2sw} - pCO_{2atm}$) in the NNS were 281 µatm and -81 µatm, respectively (Table 1, Fig. 7). From 2001 to 2011, mean surface pCO_2 increased by 75 µatm and although this region acted as a sink for all four years (negative ΔpCO_2), ΔpCO_2 increased by 53.2 µatm to -27.8 µatm in 2011, indicating a reduction in CO_2 sink capacity. Conversely, the SNS acted as a consistent summertime source of CO_2 during the 2001-2011 decade (Table 1). With the exception of a marginal decrease of 2 µatm in pCO_2 between 2001 and 2005, the SNS was analogous to the NNS in that the mean pCO_2 and ΔpCO_2 increased throughout the decade, by 37 µatm and 15.7 µatm, respectively. The apparent increase in ΔpCO_2 indicates an enhancement of this region as a source of CO_2.

Normalising these data to a temperature of 16 °C (see methods Section 2.2.7) amplifies the pCO_2 and ΔpCO_2 trends in both regions. In the NNS, surface $npCO_2$ increased by 107 µatm over the decade. Despite an interim decrease between the years of 2005 (mean $\Delta npCO_2$ = -17.5 µatm) and 2008 (mean $\Delta npCO_2$ = -27.5 µatm), we find an increase in $\Delta npCO_2$, from -71.7 µatm in 2001 to +13.4 µatm in 2011, indicating that if the SST had been 16 °C, the NNS would have switched from CO_2 sink (undersaturation) to source (supersaturation). In the SNS, we find an increase of +58 µatm in $npCO_2$ and of 36.9 µatm in $\Delta npCO_2$ from 2001-2011, with both increasing steadily between years (Table 1).

Given that ΔpCO_2 drives the air-sea CO_2 flux, it is not surprising that a comparison of the average CO_2 flux (see calculations Section 2.2.8) indicates that the NNS acted as a sink for pCO_2 and the SNS as a source (Fig. 8). From 2001-2008, the NNS average CO_2 flux exceeded that of the SNS, such that the entire North Sea acted as a weak sink for CO_2, as previously described in the literature (Bozec et al., 2005). However, in 2011, the comparatively large average CO_2 flux in the SNS of 2.23 mmol m^{-2} d^{-1} exceeded that of the NNS (-1.87 mmol m^{-2} d^{-1}) in magnitude, resulting in net positive flux, and a resultant switch to the North Sea basin acting as a source of pCO_2 to the atmosphere (Fig. 8(a)).

Due to the method used to determine biological flux (see Section 2.2.8, method (iii)) we can directly compare it to our estimated average CO_2 flux (Fig. 8(a), (b)). We find that in the NNS, biological activity constituted a significant proportion of the average CO_2 flux: 29 % in 2001; 42 % in 2005; 40 % in 2008; and 19 % in 2011. All aforementioned fluxes were indicative of primary production, enabling a distinction of the net effect of biology. However, in the SNS, whilst the biological flux is also indicative of primary production, the average CO_2 flux is positive (CO_2 source), therefore other processes counteract the biological effect in this region. For comparison the biological

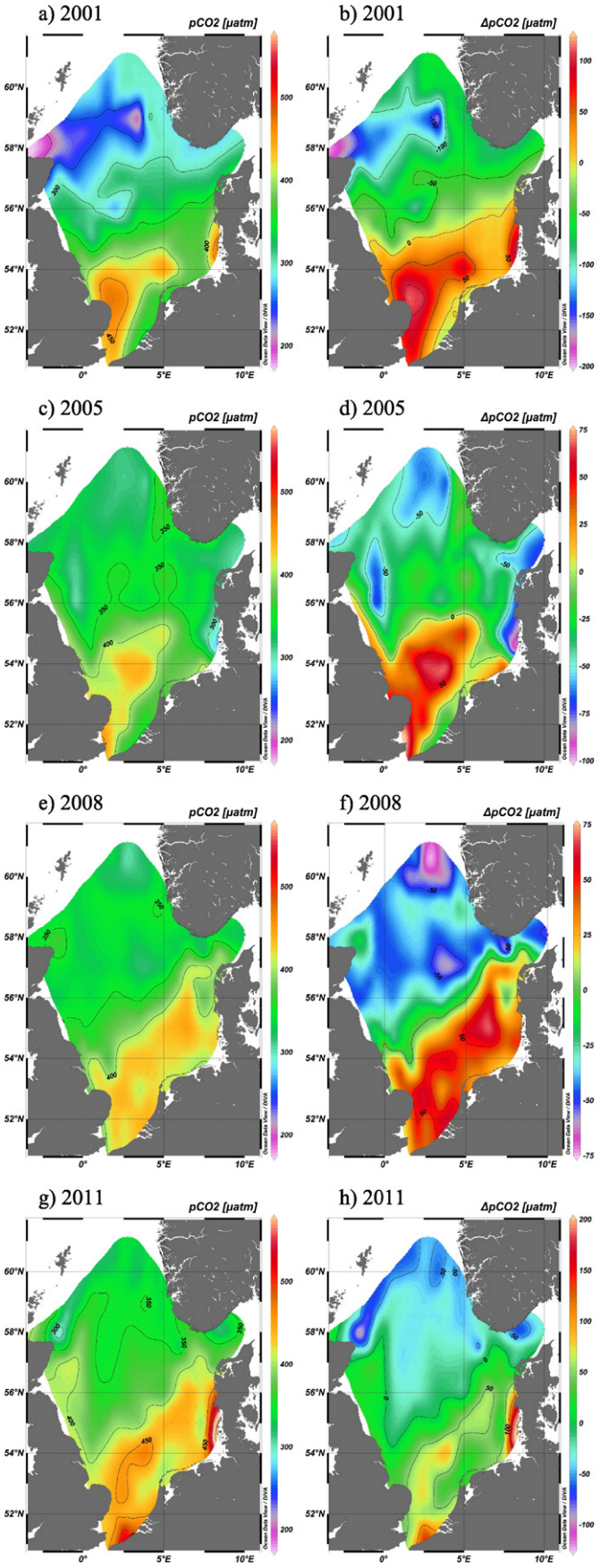

flux and average CO_2 flux calculated for each year were: 0.37 and -0.37 mmol m^{-2} d^{-1} for 2001; 0.74 and -0.19 mmol m^{-2} d^{-1} for 2005, 0.35 and -0.56 mmol m^{-2} d^{-1} for 2008 and 0.41; and -2.23 mmol m^{-2} d^{-1} for 2011.

By plotting the anomalies of the calculated npCO_2 flux it is apparent that from 2001-2008, temperature had a positive effect (greater outgassing) on flux direction, in both the NNS and SNS. However, in 2011, the temperature-normalised flux anomaly had a comparatively large negative value, indicative of enhanced uptake of CO_2, again within both regions of the North Sea. Whilst the wind-averaged flux anomaly was variable in the SNS, a clear decreasing trend over the 2001-2011 decade is evident throughout the basin (Fig. 8(b)) and in the NNS (Fig. 8(c)).

4. Discussion

4.1. DIC

Over the 2001-2011 decade we observe a substantial increase in surface DIC_{obs} in both regions of the North Sea, which leads us to investigate the cause, and more specifically if it is the result of a long-term trend due to anthropogenic CO_2 emissions, or merely the expression of natural variability. Of the factors influencing DIC in the North Sea we further consider biological activity, i.e. photosynthesis and remineralisation, and CO_2 gas exchange across the air-sea interface. Given that fluvial input constitutes 0.7 % of the carbon budget of the North Sea basin (Thomas et al., 2005b), we will assume that the variability of the fluvial effects on DIC_{obs} over the 2001-2011 decade is negligible for the purpose of this study. We also assume that lateral advection of water from the North Atlantic is comparable between years, as Salt et al. (2013) found that the contribution of this water mass varied by only 3 % from 2001- 2008. However, given the large volumes of water involved, further studies are required to deepen our understanding of this process.

During late summer, the time of observations, both primary production and remineralisation are significant ongoing processes (Bozec et al., 2005; 2006; Schiettecatte et al., 2007), thus making an assessment of anthropogenically-driven change complicated. In an attempt to differentiate between the contribution of the atmosphere and biological processes, we have calculated DIC_{bio}. However, it has been previously noted that in the North Sea, changes in the end members of its constituent water masses can also significantly impact the carbonate system (Thomas et al., 2008; Salt et al., 2013). To account for any water mass changes we use DIC_{base} which shows that in the NNS from 2001 to 2005, the average *background* DIC increased by 9 µmol kg^{-1} and from 2005 to 2008 it decreased by 2 µmol kg^{-1}. These values are consistent with trends in DIC_{atm} (calculated effect of atmospheric pCO_2 on DIC, see Section 2.2.4) of $+13 \pm 3$ µmol kg^{-1} from 2001 to 2005 and -7 $\pm$ 3 µmol kg^{-1} from 2005 to 2008, and fall within our error estimates. As such, during these two time periods we see no significant evidence in the NNS of additional DIC from different North Sea water masses. In contrast to this, from 2008 to 2011, a theoretical atmospheric driven increase in DIC_{atm} of $+15$ µmol kg^{-1} is calculated; however, we observe a decrease of 20 µmol kg^{-1} in DIC_{base}. In 2011, the water column inventory of AOU of the NNS (not shown) and at our representative station (60 mmol m^{-3}), is higher than in previous years, indicating that there is a greater amount of remineralisation taking place. This is supported by an increase in mean water column DIC_{obs} of 6 µmol kg^{-1} in the subsurface layer (not shown).

Fig. 7. Basin-wide surface distributions of gridded pCO_2: a) 2001 c) 2005 e) 2008 and g) 2011, and ΔpCO_2: b) 2001 d) 2005 f. 2008 and h) 2011. Please note the different scales for ΔpCO_2. This plot was created using Ocean Data View (Schlitzer, R., Ocean Data View, http://odv.awi.de, 2015), using DIVA gridding with an automatic scale length: X-scale-length [permille]= 22; Y scale-length [permille].

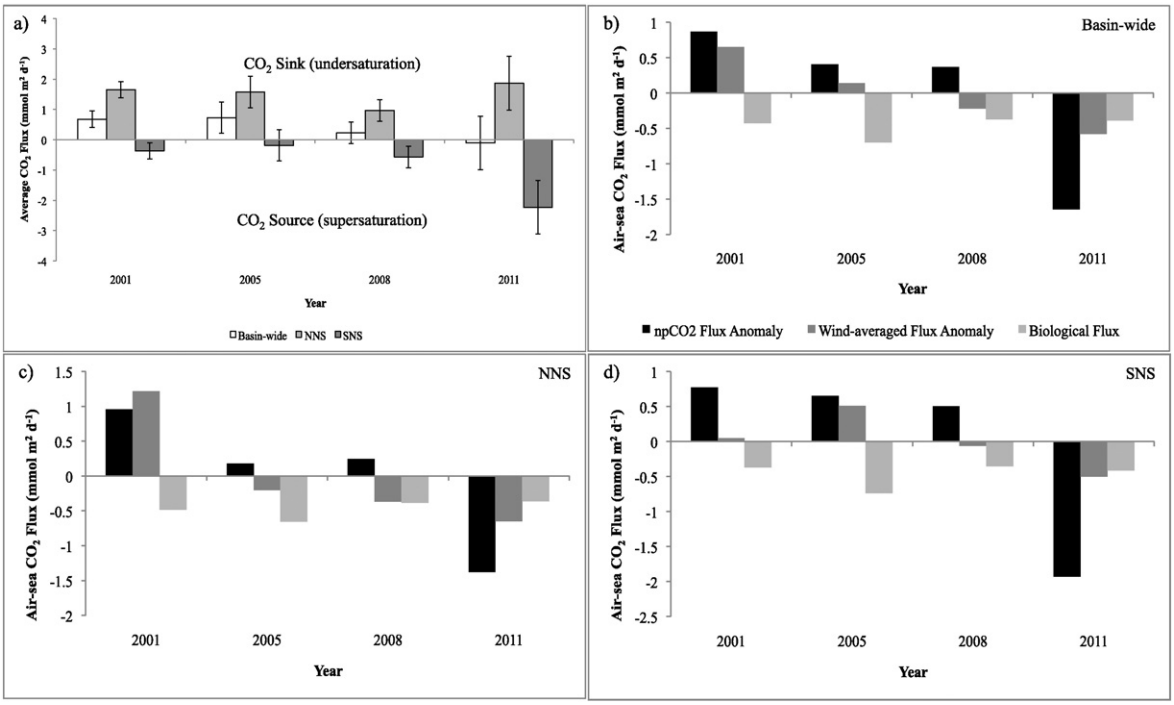

Fig. 8. Air-sea CO_2 fluxes: a) Basin-wide, NNS, and SNS average CO_2 flux b) Comparison of basin-wide mean npCO_2 and wind-averaged flux anomalies and biological flux c) Comparison of NNS mean npCO_2 and wind-averaged flux anomalies and biological flux d) Comparison of SNS mean npCO_2 and wind-averaged flux anomalies and biological flux.

A contributing factor that could lead to elevated DIC_{obs} in 2011 compared to other years is the presence of a weaker anti-clockwise circulation within the North Sea. Salt et al. (2013) found that the strength of the shelf pump of CO_2 is enhanced in years of positive North Atlantic Oscillation Index (NAOI), and we suggest that here we see the opposite effect during negative NAOI conditions (winter (DJFM) NAOI was -1.9, 0.12, 2.1 and -1.57, for 2001, 2005, 2008 and 2011, respectively (https://climatedataguide.ucar.edu/climate-data/hurrell-north-atlantic-oscillation-nao-index-station-based, 2015). A weaker circulation would result in a higher proportion of metabolic DIC outgassing to the atmosphere as opposed to being transported into the North Atlantic. This is supported by the reduction in biological pCO_2 flux in the surface layer (19 % in 2011) and by a higher water column inventory of AOU (Fig. 6(b)) and DIC_{obs} (Fig. 6(a)) in 2011, as evident at our representative NNS station, in comparison to other years.

In contrast to the NNS, DIC_{base} in the SNS shows consistent behaviour indicating a steady-state. Fig. 5 (DIC_{bio}) shows that remineralisation dominates the DIC_{bio} signal in the SNS in August, leading to elevated DIC_{obs} compared to the NNS. As we have shown that DIC_{base} in the SNS does not vary significantly, one would expect the increases in surface DIC_{obs} to be driven by a combination of biological activity and exchange with the atmosphere.

4.2. pCO_2

The average CO_2 flux calculations for each region indicate that for all years, the SNS acted as a summertime source of CO_2 to the atmosphere (CO_2 outgassing, negative CO_2 flux) whilst the NNS acted as a sink (CO_2 invasion, positive CO_2 flux) (Fig. 8(a)). This summertime distinction between the supersaturated SNS and undersaturated NNS has been well described in the literature (Thomas et al., 2004; 2005a; Bozec et al., 2005, Schiettecatte et al., 2007; Prowe et al., 2009) and has also been reported in other coastal regions, which show a divide between stratified and mixed systems (Marrec et al., 2013). Over the 2001- 2011 decade, the ΔpCO_2 in the NNS becomes less negative (i.e. weaker undersaturation). However, this appears to have no impact on the average CO_2 flux which we find, with the exception of 2008, where the mean was at a minimum (0.97 ± 0.36 mmol m^{-2} d^{-1}), to be relatively consistent at 1.65 ($\pm$ 0.27), 1.58 ($\pm$ 0.52), and 1.87 ($\pm$ 0.89) mmol m^{-2} d^{-1} in 2001, 2005 and 2011, respectively. We do note that a mean positive (and therefore supersaturated) $\Delta npCO_2$ of 13.4 μatm was calculated for the NNS in 2011, indicating that if the sea surface temperatures had not been as cold as those observed during 2011 (Table 1), the NNS could have acted as a summertime source of CO_2 to the atmosphere, a situation that to our knowledge, has not been observed before. As yet this phenomenon has not impacted upon the direction of the average CO_2 flux for this region; indeed it remained positive (indicating undersaturation) throughout the decade, therefore the NNS acted as a consistent sink for atmospheric CO_2.

Our estimated average CO_2 fluxes are somewhat lower than the summertime flux of 2.4 to 3.8 mmol m^{-2} d^{-1} calculated by Bozec et al. (2005) for the NNS and - 4.2 ($\pm$ 0.2) mmol m^{-2} d^{-1} calculated by Schiettecatte et al. (2007) for the SNS, both of whom used pCO_2 measurements for their calculations, in contrast to the calculated pCO_2 used here. We account for this difference in our error calculations, following a study of the internal consistency of the carbon system in the North Sea by Salt et al. (2015), see Sections 2.2.2 and 2.2.4. We therefore propose that differences in the flux estimates may be the result of a combination of the following: interannual variability; our use of monthly-averaged wind speed data as opposed to the high resolution datasets used by other studies; and the varying definitions of geographic areas: Bozec et al. (2005) divide the NNS and SNS at 54 °N, compared to 56 °N here, and Schiettecatte et al. (2007) focus on the smaller area of the Southern Bight.

In contrast to the NNS, from 2001-2008 the average CO_2 fluxes in the SNS were variable (-0.37, -0.19, and -0.56 mmol m^{-2} d^{-1} in 2001, 2005 and 2008, respectively), and again lower than the flux of Bozec et al. (2005) (-0.8 to -1.7 mmol m^{-2} d^{-1}). In 2011 we find a substantial increase in average CO_2 flux (-2.23 ± 0.88 mmol m^{-2} d^{-1}), exceeding the upper limit of the flux estimates by Bozec et al. (2005) but still smaller than estimated by Schiettecatte et al. (2007) for the Southern Bight. Therefore in 2011 the SNS acted as a strong source of CO_2 to the atmosphere, relative to the previous years of our study. This is reflected in the mean ΔpCO_2, which becomes more positive over the 2001-2011

(i.e. increase in the difference between pCO_{2sw} and pCO_{2atm} and stronger supersaturation), and indicates that the SNS became a stronger source of CO_2 over the progression of the 2001-2011 decade. The effect of temperature normalisation is evident in a comparison of the mean ΔpCO_2 and $\Delta npCO_2$ in this region; in 2001 and 2008, when mean SST >16 °C, normalising the pCO_2 data to 16 °C resulted in less positive $\Delta npCO_2$ than ΔpCO_2, i.e. weaker supersaturation. The opposite is true for 2005 and 2011. During these summers mean SST <16 °C, thus normalising the pCO_2 data led to an increase from ΔpCO_2 to $\Delta npCO_2$, representative of stronger supersaturation. On a basin-wide scale, with the exception of 2001, where there is little difference between ΔpCO_2 and $\Delta npCO_2$, attributable to the aforementioned high SST in the SNS, $\Delta npCO_2$ is less negative than ΔpCO_2 in 2005 and 2008, indicative of weaker undersaturation, and more positive in 2011, indicative of stronger supersaturation.

By investigating the components that either dampen or enhance the CO_2 flux (Fig. 8(b), (c), (d)) we find that primary productivity accounts for a significant proportion of the NNS average CO_2 flux, as observed previously (Prowe et al., 2009), however the biological flux shows relatively little variation between years, with uptake ranging from 0.36 to 0.65 mmol m^{-2} d^{-1}). In stark contrast to this, we find that temperature effects show significant inter-annual variability within both regions of the North Sea. The impact of temperature on CO_2 fluxes was largest in 2011, which was also the year that we observed the greatest difference in mean temperature between the NNS and SNS and the largest difference in average CO_2 flux between the two regions in all four years. We also find that the wind component in the NNS appears to decrease over the 2001-2011 decade. This may be partly due to changes in the timing of our observational window, or to variability of wind velocity at seasonal and decadal timescales.

With the predicted rises in global sea surface temperature (SST) (Rhein et al., 2013) it is possible that summertime SST in the NNS could rise sufficiently to cause the region to switch from undersaturation (CO_2 sink) to supersaturation (CO_2 source). This is evident in our calculations of ΔpCO_2 and $\Delta npCO_2$ in the NNS in 2011 (see Table 1), which are -27.8 μatm and 13.4 μatm, respectively. As previously mentioned, mean SST was particularly low in the summer of 2011 (13.3 °C), therefore our calculations indicate that if the SST in the NNS had been 16 °C, the ΔpCO_2 would have been positive, and average CO_2 flux would have been negative (CO_2 source). Coupled with the potential strengthening of the SNS as a source of CO_2, as indicated by a more positive $\Delta npCO_2$ than ΔpCO_2 in this region in 2011, this could result in a basin-wide reduction of CO_2 drawdown, which in turn may have potential ramifications for the efficiency of the North Sea as a continental shelf pump with respect to CO_2.

4.3. Implications of rapidly increasing surface DIC and pCO_2

Regardless of the causal factors, the observed rapid increases in DIC and pCO_2 over the 2001-2011 decade have implications for the chemical composition of the North Sea. Here we investigate pH and buffering capacity, which is described by the Revelle factor:

$$\text{R.F.} = (\delta CO_2/CO_2)/(\delta DIC/DIC) \quad (6)$$

which is the relative change of surface water pCO_2 divided by the ensuing relative change of DIC in surface waters. With the increasing CO_2 in the atmosphere in our era, the R.F. tends to increase, i.e. the buffer capacity tends to decrease over the years. The underlying mechanism relates to the decreasing availability of the carbonate ion (CO_3^{2-}) for the formation of bicarbonate ions (HCO_3^-) when CO_2 reacts with seawater. With increasing CO_2 uptake, an increase in $[CO_2]_{aq}$ results in a decrease of $[CO_3^{2-}]$, and therefore a reduction in the capacity to buffer against further CO_2 uptake, or an increased Revelle factor (Takahashi et al., 1980; Sarmiento and Gruber, 2006).

In order to evaluate the changes in the pH and the Revelle factor of the surface waters between years, we corrected for biological activity using the same method used to calculate DIC_{bio} (see Section 2.2.4), thereby using measured A_T and the atmospheric pCO_2 for each year (assuming equilibrium) to calculate abiotic pH (Table 2) and abiotic Revelle factor (Table 3).

The biogeochemical divide in the North Sea is once again evident when comparing the mean pH and Revelle factor for each region with their abiotic equivalents (see Fig. 9 and Tables 2 and 3). In the NNS, biology is dampening the effects of anthropogenic CO_2 invasion, as a net autotrophic system results in DIC uptake, causing a subsequent increase in mean pH (abiotic pH < pH) and decrease in mean Revelle factor. The opposite is true in the SNS, which is net heterotrophic, thus the effects of increasing atmospheric CO_2 are enhanced, as respiration lowers pH further (abiotic pH > pH), and results in a higher Revelle factor.

In the NNS, mean abiotic pH decreased over the 2001-2011 decade from 8.0819 to 8.0606, which corresponds to an annual increase in $[H^+]$ of 4.1630 x 10^{-11} mol yr^{-1}. At a pH level of 8.0819 (2001), this corresponds to a pH change of -0.0022 pH units yr^{-1}. In the SNS, mean abiotic pH decreased from 8.0859 to 8.0638, which corresponds to an annual increase in $[H^+]$ of 4.2840 x 10^{-11} mol yr^{-1}. This results in a comparable pH change of 0.0023 pH units yr^{-1}, from a pH of 8.0859 (2001) (Table 2). This is not altogether surprising given that a basin-wide atmospheric pCO_2 was used to calculate abiotic pH. These rates do compare well with the trends observed in seven CO_2 system time-series studies in various locations, reported by Bates et al. (2014), in particular with the rate of -0.0026 pH units yr^{-1} observed in the Irminger Sea, and with the pH decline of 0.002 pH units yr^{-1} simulated by Lorkowski et al. (2012).

For comparison (Fig. 9), without discounting biological activity, mean pH in the NNS decreased over the 2001-2011 decade from 8.1781 to 8.0904, which corresponds to an annual increase in $[H^+]$ of 1.4849 x 10^{-10} mol yr^{-1}, corresponding to a pH change of -0.0096 units yr^{-1} from a starting pH of 8.1781 (2001). In the SNS, mean pH decreased from 8.0715 to 8.0344, which corresponds to an annual increase in $[H^+]$ of 7.5650 x 10^{-11} mol yr^{-1}, resulting in a pH change of -0.0039 pH units yr^{-1}, from a pH of 8.0715 (2001) (Table 2).

Furthermore, as a result of increasing surface DIC, and despite the removal of biological effects, we calculate a decadal reduction in the buffering capacity (increasing Revelle factor, see Table 3) of the surface waters of the North Sea, which is to be expected given the continued invasion of atmospheric CO_2. As atmospheric pCO_2 continues to rise, the reduction of the buffering capacity will accelerate, as model studies have shown that at higher Revelle factors, despite a constant rise in atmospheric pCO_2, less DIC and therefore a reduced CO_2 flux is required to reach equilibrium between surface waters and the overlying air (Thomas et al., 2007, Lorkowski et al., 2012). This could further explain the consistent increase in ΔpCO_2 calculated in the NNS.

In contrast, in the supersaturated SNS, the secular trend of rising atmospheric pCO_2 should lead to a reduction in ΔpCO_2, yet we see the opposite. Several processes can be thought of, which may contribute to this observed scenario. The overall rising SST (Rhein et al., 2013) would raise the surface water pCO_2, although this signal can be overridden sporadically by shorter-term variability. Furthermore, the reduction in fluvial input of nitrate to the North Sea since the late 1990's (Provoost et al., 2010; Borges and Gypens, 2010) could lead to a decrease in CO_2 fixation in the SNS, and in turn would shift the trophic balance further toward heterotrophy, thus higher surface water pCO_2. As discussed in Burt et al. (2015), the recent reduction of fluvial nitrate input also has the potential to diminish the release of respiratory A_T, which in turn would result in a stronger decline in pH, than that which would occur purely due to atmospheric pCO_2 increase. This scenario is depicted in our comparison of pH and abiotic pH in this region (pH < abiotic pH) (see Table 2, Fig. 9(c), (d)). Similarly, for a given level of heterotrophy and associated metabolic DIC release, a reduction in A_T would result in an increase in pCO_2, with a subsequent increase in ΔpCO_2 and a

Table 2
Mean values of pH and abiotic pH, with corresponding changes to $[H^+]$ and calculated rates of change of pH and Revelle factor for the North Sea basin (based on 262 data points), the NNS (136 data points) and SNS (126 data points), using gridded surface data (< 10 m). All abiotic parameters are calculated using A_T and pCO_{2atm}, thus assuming equilibrium. All parameters are quoted with calculation error (CE) as outlined in Section 2.2.2, with CE averaged between comparable years and divided by the number of years to estimate error for the rate of change.

Year	pH	Corresponding $[H^+]$ (mol)	Difference in $[H^+]$ (mol)	Rate of change of $[H^+]$ (mol yr^{-1})	Change in $[H^+]$ from 2001 to 2011 (mol)	Corresponding pH change from 2001 (units yr^{-1})
Basin-wide						
2001	8.1268 ± 0.0092	7.4679 x 10^{-9}				
2005	8.0937 ± 0.0093	8.0593 x 10^{-9}	5.9140 x 10^{-10}	1.4785 x 10^{-10}		
2008	8.0788 ± 0.0078	8.3407 x 10^{-9}	2.8140 x 10^{-10}	9.3800 x 10^{-11}		
2011	8.0635 ± 0.0066	8.6397 x 10^{-9}	2.9900 x 10^{-10}	9.9667 x 10^{-11}	1.1718 x 10^{-9}	-0.0068
NNS (>56 °N)						
2001	8.1781 ± 0.0092	6.6359 x 10^{-9}				
2005	8.1142 ± 0.0093	7.6878 x 10^{-9}	1.0519 x 10^{-9}	2.6298 x 10^{-10}		
2008	8.1050 ± 0.0078	7.8524 x 10^{-9}	1.6460 x 10^{-10}	5.4867 x 10^{-11}		
2011	8.0904 ± 0.0066	8.1208 x 10^{-9}	2.6840 x 10^{-10}	8.9467 x 10^{-11}	1.4849 x 10^{-9}	-0.0096
SNS (<56 °N)						
2001	8.0715 ± 0.0092	8.4820 x 10^{-9}				
2005	8.0716 ± 0.0093	8.4801 x 10^{-9}	-1.9000 x 10^{-12}	-4.7500 x 10^{-13}		
2008	8.0504 ± 0.0078	8.9043 x 10^{-9}	4.2420 x 10^{-10}	1.4140 x 10^{-10}		
2011	8.0344 ± 0.0066	9.2385 x 10^{-9}	3.3420 x 10^{-10}	1.1140 x 10^{-10}	7.5650 x 10^{-10}	-0.0039
Year	Abiotic pH	Corresponding $[H^+]$ (mol)	Difference in $[H^+]$ (mol)	Rate of change of $[H^+]$ (mol yr^{-1})	Change in $[H^+]$ from 2001 to 2011 (mol)	Corresponding pH change from 2001 (units yr^{-1})
Basin-wide						
2001	8.0837 ± 0.0004	8.2471 x 10^{-9}				
2005	8.0729 ± 0.0004	8.4547 x 10^{-9}	2.0760 x 10^{-10}	5.1900 x 10^{-11}		
2008	8.0682 ± 0.0002	8.5467 x 10^{-9}	9.2000 x 10^{-11}	3.0667 x 10^{-11}		
2011	8.0620 ± 0.0001	8.6696 x 10^{-9}	1.2290 x 10^{-10}	4.0967 x 10^{-11}	4.2250 x 10^{-10}	-0.0022
NNS (>56 °N)						
2001	8.0819 ± 0.0004	8.2813 x 10^{-9}				
2005	8.0716 ± 0.0004	8.4801 x 10^{-9}	1.9880 x 10^{-10}	4.9700 x 10^{-11}		
2008	8.0674 ± 0.0002	8.5625 x 10^{-9}	8.2400 x 10^{-11}	2.7467 x 10^{-11}		
2011	8.0606 ± 0.0001	8.6976 x 10^{-9}	1.3510 x 10^{-10}	4.5033 x 10^{-11}	4.1630 x 10^{-10}	-0.0022
SNS (<56 °N)						
2001	8.0859 ± 0.0004	8.2054 x 10^{-9}				
2005	8.0745 ± 0.0004	8.4236 x 10^{-9}	2.1820 x 10^{-10}	5.4550 x 10^{-11}		
2008	8.0691 ± 0.0002	8.5290 x 10^{-9}	1.0540 x 10^{-10}	3.5133 x 10^{-11}		
2011	8.0638 ± .0001	8.6338 x 10^{-9}	1.0480 x 10^{-10}	3.4933 x 10^{-11}	4.2840 x 10^{-10}	-0.0023

strengthening of the supersaturation of the SNS, just as we observe in the 2001-2011 decade. Future research is required to monitor the A_T signal over seasonal cycles and at a higher resolution in order to investigate this further.

Once the biological signal is removed, we observe the effects of increasing atmospheric pCO_2 throughout the North Sea, as increasing $[H^+]$ (decreasing pH) and $[HCO_3^-]$, with concurrent decreases in $[CO_3^{2-}]$, $\Omega_{Calcite}$ and $\Omega_{Aragonite}$ (Table 3). This phenomenon, termed "Ocean acidification" is well documented, the effects of which are multifaceted. Changing pH may affect the speciation of other chemical constituents of seawater, including bio-essential trace-elements, such as iron (Millero et al., 2009). Decreasing $\Omega_{Calcite}$ and $\Omega_{Aragonite}$ impacts marine

Table 3
Mean values of Revelle factor and abiotic parameters for the North Sea basin (based on 262 data points), the NNS (136 data points) and SNS (126 data points), using gridded surface data (< 10 m). All abiotic parameters are calculated using A_T and pCO_{2atm}, thus assuming equilibrium. All parameters are quoted with calculation error (CE) as outlined in Section 2.2.2, with CE averaged between comparable years and divided by the number of years to estimate error for the rate of change.

Year	Revelle Factor	Rate of change in Revelle Factor (yr^{-1})	Abiotic Revelle Factor	Abiotic $[CO_3^{2-}]$ (μmol kg^{-1})	Abiotic $[HCO_3^-]$ (μmol kg^{-1})	Abiotic $\Omega_{Calcite}$	Abiotic $\Omega_{Aragonite}$
Basin-wide							
2001	10.511 ± 0.12		11.012 ± 0.001	171.4 ± 0.4	1871.6 ± 2.2	4.11 ± 0.01	2.64 ± 0.01
2005	11.022 ± 0.13	+ 0.128 ± 0.033	11.309 ± 0.001	164.4 ± 0.3	1893.1 ± 2.2	3.93 ± 0.01	2.52 ± 0.01
2008	11.053 ± 0.11	+ 0.01 ± 0.04	11.192 ± 0.001	166.9 ± 0.2	1882.7 ± 1.5	4.00 ± 0.01	2.57 ± 0.003
2011	11.584 ± 0.09	+ 0.177 ± 0.033	11.617 ± 0.0002	156.9 ± 0.1	1905.3 ± 0.8	3.76 ± 0.002	2.41 ± 0.001
NNS (>56 °N)							
2001	10.038 ± 0.12		11.179 ± 0.001	165.9 ± 0.4	1875.8 ± 2.2	3.97 ± 0.01	2.55 ± 0.01
2005	10.934 ± 0.13	+ 0.224 ± 0.033	11.502 ± 0.001	158.9 ± 0.3	1897.1 ± 2.2	3.80 ± 0.01	2.44 ± 0.01
2008	10.858 ± 0.11	-0.025 ± 0.04	11.332 ± 0.0005	162.9 ± 0.2	1883.3 ± 1.5	3.91 ± 0.01	2.51 ± 0.003
2011	11.48 ± 0.09	+ 0.207 ± 0.033	11.878 ± 0.0002	150.2 ± 0.1	1910.9 ± 0.8	3.60 ± 0.002	2.3 ± 0.001
SNS (<56 °N)							
2001	11.022 ± 0.12		10.807 ± 0.001	178.2 ± 0.4	1866.5 ± 2.2	4.28 ± 0.01	2.75 ± 0.01
2005	11.118 ± 0.13	+ 0.024 ± 0.033	11.073 ± 0.001	171.1 ± 0.3	1888.3 ± 2.2	4.09 ± 0.01	2.63 ± 0.01
2008	11.264 ± 0.11	+ 0.049 ± 0.04	11.021 ± 0.0005	171.8 ± 0.2	1881.9 ± 1.5	4.11 ± 0.01	2.65 ± 0.003
2011	11.697 ± 0.09	+ 0.144 ± 0.033	11.298 ± 0.0002	165.1 ± 0.1	1898.6 ± 0.8	3.95 ± 0.002	2.54 ± 0.001

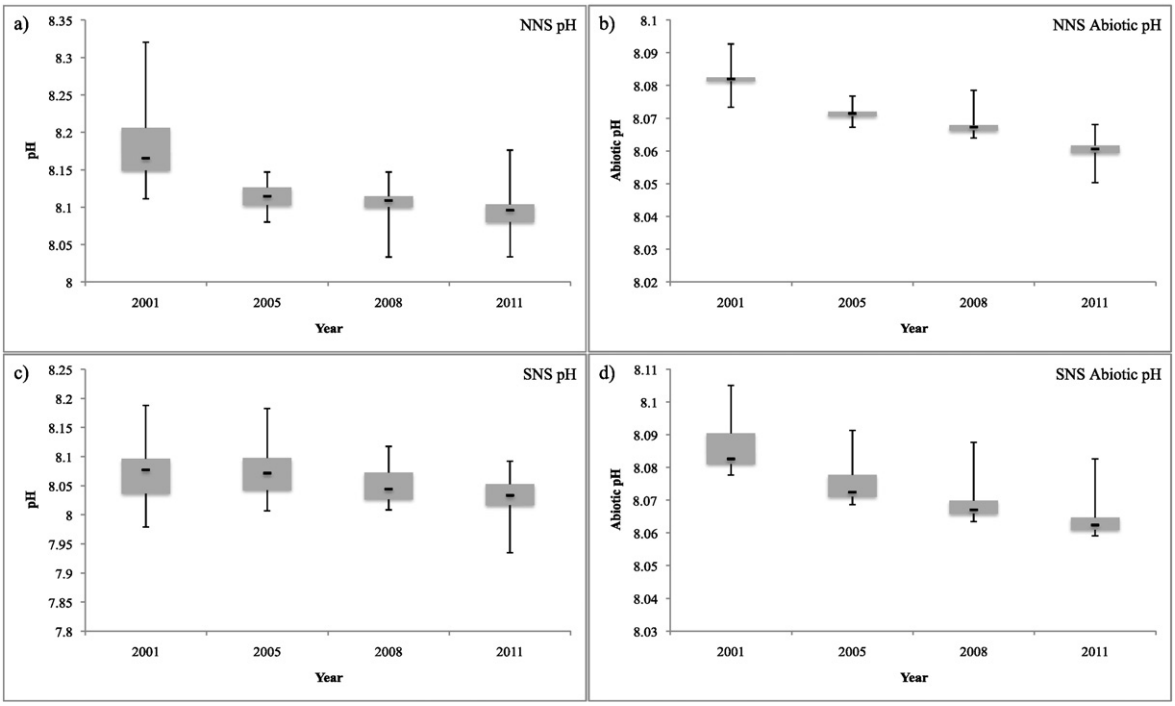

Fig. 9. Box and Whisker plots using the same data as displayed in Table 2, for a) NNS pH b) NNS abiotic pH c) SNS pH d) SNS abiotic pH. Please note the differences in scale between each plot. Median values are indicated by the horizontal black lines inside each box; the boxes span the interquartile range and the whiskers indicate variability outside the upper and lower quartiles.

organisms that form calcareous shells. Many calcifying species exhibit reduced calcification in laboratory experiments under high-CO_2 conditions (Doney et al., 2009). Notably shellfish calcification was found to decrease in experiments (Gazeau et al., 2007). The manifestations of these impacts are potentially ecosystem-wide, which could be of particular concern in regions of high economic importance, such as shelf seas, with commercially important fisheries, as for example, the extensive shellfish populations and shellfish fisheries found in the North Sea region.

If, as projected, atmospheric pCO_2 continues to rise, it is possible that the synergistic effects of a decline in buffering capacity and rising SST could lead to a reduction in the efficiency of the North Sea as a CO_2 sink, and subsequently as a continental shelf pump. Given that the estimated net uptake of coastal and marginal seas is 20 % of the ocean's capacity for CO_2 storage (Thomas et al., 2004), the occurrence of a similar phenomenon in other shelf-pump regions could have significant negative impacts on the capacity of the oceans to mitigate anthropogenically-induced climate change.

5. Concluding remarks

Here we present observational evidence that suggests that DIC and pCO_2 in the surface waters of the North Sea basin are increasing at a rate that is faster than concurrent increases in atmospheric pCO_2. However, upon further investigation we conclude that these observations are largely the result of biological activity, masking the signal of increasing CO_2 concentrations that mirror those in the atmosphere due to anthropogenic input. We find that biological activity mitigates rising atmospheric pCO_2 in the NNS, and enhances its effects in the SNS. We suggest a complex interplay exists between the effects of climate change and variability in both biological activity and terrestrial influence of coastal systems.

Furthermore, we propose that the synergistic effects of biological activity, terrestrial influences, and a reduction in buffering capacity due to the invasion of increasing atmospheric CO_2, coupled with projected rises in SST, are not only causing a reduction in pH, but also a weakening of the undersaturation of the NNS and a strengthening of the supersaturation of the SNS. In a future with higher SST and higher atmospheric pCO_2, this may lead to a significant switch in the NNS from a summertime sink to a source of CO_2 with potentially important ramifications for the efficiency of the North Sea as a continental shelf pump for CO_2. A resultant reduction in the transport of CO_2 to intermediate waters of the North Atlantic would generate a positive feedback loop due to a reduced capacity of the North Sea basin to mitigate the continuing rise in atmospheric pCO_2.

The continued assessment of the North Sea carbon system would further facilitate the quantification of multi-annual versus long-term trends. Further investigations into other important continental shelf pumps of other coastal seas around the world are required to assess the state of their efficiency and ability to mitigate the continuing rise in atmospheric pCO_2.

Acknowledgments

We would like to take the opportunity to thank the captains and crews of the R.V. Pelagia, the nutrients group at NIOZ, and the two anonymous reviewers for their constructive comments that helped to improve this paper. We gratefully acknowledge the data produced in all four cruises by several colleagues, at the time working at NIOZ, as well as by Dr. Alberto Borges and his colleagues at the Chemical Oceanography Unit, University of Liège. This program was supported by the National Programme for Sea and Coastal Research (ZKO) of the Netherlands Organisation for Scientific Research (NWO) and CARBOOCEAN.

References

Anderson, L.A., Sarmiento, J.L., 1994. Redfield Ratios of remineralisation determined by nutrient data analysis. Glob. Biogeochem. Cycles 8, 65–80.

Bates, N.R., Astor, Y.M., Church, M.J., Currie, K., Dore, J.E., González-Dávila, M., Lorenzoni, L., Muller-Karger, F., Olafsson, J., Santana-Casiano, J.M., 2014. A time-series view of changing surface ocean chemistry due to ocean uptake of anthropogenic CO_2 and ocean acidification. Oceanography 27 (1), 126–141.

Borges, A.V., Gypens, N., 2010. Carbonate chemistry in the coastal zone responds more strongly to eutrophication than to ocean acidification. Limnol. Oceanogr. 55, 346–353.

Borges, A.V., 2011. Present Day Carbon Dioxide Fluxes in the Coastal Ocean and Possible Feedbacks Under Global Change. In: Duarte, P., Santana-Casiano, J.M. (Eds.), Oceans and the Atmospheric Carbon Content. Springer Science + Business Media B.V., pp. 47–77.

Bozec, Y., Thomas, H., Elkalay, K., de Baar, H.J.W., 2005. The continental shelf pump for CO_2 in the North Sea - evidence from summer observations. Mar. Chem. 93, 131–147.

Bozec, Y., Thomas, H., Schiettecatte, L.-S., Borges, A.V., Elkalay, K., de Baar, H.J.W., 2006. Assessment of the processes controlling the seasonal variations of dissolved inorganic carbon in the North Sea. Limnol. Oceanogr. 51, 2746–2762.

Burt, W.J., Thomas, H., Hagens, M., Pätsch, J., Clargo, N.M., Salt L, A., Winde, V., Böttcher, M.E., 2015. Evaluating North Sea carbon sources using radium and stable carbon isotope ($\delta^{13}C_{DIC}$) tracers. Limnol. Oceanogr. (2015). (in revision).

Chen, C.-T.A., Borges, A.V., 2009. Reconciling opposing views on carbon cycling in the coastal ocean: Continental shelves as sinks and near-shore ecosystems as sources of atmospheric CO2. Deep-Sea Res. II 56, 578–590.

Dickson, A.G., Millero, F.J., 1987. A comparison of the equilibrium constants for the dissociation of carbonic acid in seawater media. Deep-Sea Res. 34 (10), 1733–1743.

Dickson, A.G., Sabine, C.L., Christian, J.R. (Eds.), 2007. Guide to Best Practices for Ocean CO_2 Measurements. PICES Special Publication 3 191 pp.

Doney, S.C., Fabry, V.J., Feely, R.A., Kleypas, J.A., 2009. Ocean Acidification: The Other CO_2 Problem. Ann. Rev. Mar. Sci. 1, 169–192.

Gattuso, J.-P., Frankignoulle, M., Wollast, R., 1998. Carbon and carbonate metabolism in coastal aquatic ecosystems. Annu. Rev. Ecol. Syst. 29, 405–434.

Gazeau, F., Quiblier, O., Jansen, J., Gattuso, J.P., Middelburg, J.J., Heip, C., 2007. Impact of elevated CO_2 on shellfish calcification. Geophys. Res. Lett. http://dx.doi.org/10.1029/2006GL02855.

van Heuven, S., Pierrot, D., Lewis, E., Wallace, D.W.R., 2011. MATLAB Program Developed for CO_2 System Calculations. ORNL/CDIAC-105b. Carbon Dioxide Information Analysis Centre, Oak Ridge National Laboratory, U.S. Department of Energy, Oak Ridge, Tennessee.

ICES, 1983. International Council for the Exploration of the Sea: Flushing times of the North Sea. ICES Cooperative Research Report 123.

Kalnay, E., Kanamitsu, M., Kistler, R., Collins, W., Deaven, D., Gandin, L., Iredell, M., Saha, S., White, G., Woollen, J., Zhu, Y., Chelliah, M., Ebisuzaki, W., Higgins, W., Janowlak, J., Mo, K.C., Ropelewski, C., Wang, J., Leetmaa, A., Reynolds, R., Jenne, R., Joseph, D., 1996. The NCEP/NCAR reanalysis project. Bull. Am. Meteorol. Soc. 77, 437–471.

Kempe, S., Pegler, K., 1991. Sinks and sources of CO_2 in coastal seas: the North Sea. Tellus 43B, 224–235.

Kühn, W., Pätsch, J., Thomas, H., Borges, A.V., Schiettecatte, L.-S., Bozec, Y., Prowe, F.A.E., 2010. Nitrogen and carbon cycling in the North Sea and exchange with the North Atlantic- A model study, Part II: Carbon budget and fluxes. Cont. Shelf Res. 30, 1701–1716.

Le Menn, M., 2011. About uncertainties in practical salinity calculations. Ocean Sci. 7, 651–659.

Lenhart, H.J., Radach, G., Backhaus, J.O., Pohlmann, T., 1995. Simulations of the North Sea circulation, its variability and its implementation as hydrodynamical forcing in ERSEM. Neth. J. Sea Res. 33, 271–299.

Le Quéré, C., Moriarty, R., Andrew, R. M., Peters, G. P., Ciais, P., Friedlingstein, P., Jones, S. D., Sitch, S., Tans, P., Arneth, A., Boden, T. A., Bopp, L., Bozec, Y., Canadell, J. G., Chini, L. P., Chevallier, F., Cosca, C. E., Harris, I., Hoppema, M., Houghton, R. A., House, J. I., Jain, A. K., Johannessen, T., Kato, E., Keeling, R. F., Kitidis, V., Klein Goldewijk, K., Koven, C., Landa, C. S., Landschützer, P., Lenton, A., Lima, I. D., Marland, G., Mathis, J. T., Metzl, N., Nojiri, Y., Olsen, A., Ono, T., Peng, S., Peters, W., Pfeil, B., Poulter, B., Raupach, M. R., Regnier, P., Rödenbeck, C., Saito, S., Salisbury, J. E., Schuster, U., Schwinger, J., Séférian, R., Segschneider, J., Steinhoff, T., Stocker, B. D., Sutton, A. J., Takahashi, T., Tilbrook, B., van der Werf, G. R., Viovy, N., Wang, Y.-P., Wanninkhof, R., Wiltshire, A., and Zeng, N., 2014. Global carbon budget 2014. Earth Syst. Sci. Data, 7, 47-85, doi:http://dx.doi.org/10.5194/essd-7-47-2015, 2015.

Lewis, E.L., and Wallace, D.W.R., 1998. Program developed for CO2 system calculations, ORNL/CDIAC-105. Carbon dioxide information analysis centre, Oak Ridge National Laboratory, U.S. Department of Energy, Oak Ridge.

Lorkowski, I., Pätsch, J., Moll, A., Kühn, W., 2012. Interannual variability of carbon fluxes in the North Sea from 1970 to 2006 - Competing effects of abiotic and biotic drivers on the gas exchange of CO_2. Estuar. Coast. Shelf Sci. 100, 38–57. http://dx.doi.org/10.1016/j.ecss.2011.11.037.

Marrec, P., Cariou, T., Collin, E., Durand, A., Latimer, M., Macé, E., Morin, P., Raimund, S., Vernet, M., Bozec, Y., 2013. Seasonal and latitudinal variability of the CO_2 system in the Western English Channel based on Voluntary Observing Ships (VOS) measurements. Mar. Chem. 155, 29–41.

Mehrbach, C., Culberson, C.H., Hawley, J.E., Pytkowicz, R.M., 1973. Measurement of the apparent dissociation constants of carbonic acid in seawater at atmospheric pressure. Limnol. Oceanogr. 18, 897–907.

Millero, F.J., Woosley, R., Ditrilio, B., Waters, J., 2009. Effect of Ocean Acidification on the Speciation of Metals in Seawater. Oceanography 22 (4), 72–85.

Nightingale, P.D., Malin, G., Law, C.S., Watson, A.J., Liss, P.S., Liddicoat, M.I., Boutin, J., Upstill-Goddard, R.C., 2000. In situ evaluation of air-sea gas exchange parameterizations using novel conservative and volatile tracers. Glob. Biogeochem. Cycles 14 (1), 373–387.

Omar, A.M., Olsen, A., Johannessen, T., Hoppema, M., Thomas, H., Borges, A.V., 2010. Spatiotemporal variations of fCO_2 in the North Sea. Ocean Sci. 6, 77–89.

Pätsch, J., Lorkowski, I., 2013. Comparison of two techniques to separate physical- and biological mediated pCO2 in seawater. Limnol. Oceanogr. Methods 11, 41–52.

Provoost, P., van Heuven, S., Soetaert, K., Laane, R.W.P.M., Middelburg, J.J., 2010. Seasonal and long-term changes in pH in the Dutch coastal zone. Biogeosciences 7, 3869–3878.

Prowe, A.E.F., Thomas, H., Pätsch, J., Kühn, W., Bozec, Y., Schiettecatte, L., Borges, A., de Baar, H.J.W., 2009. Mechanisms controlling the air-sea CO_2 flux in the North Sea. Cont. Shelf Res. 29, 1801–1808.

Queste, B.Y., Fernand, L., Jickells, T.D., Heywood, K.J., 2013. Spatial extent and historical context of North Sea oxygen depletion in August 2010. Biogeochemistry 113, 53–68.

Rhein, M., Rintoul, S.R., Aoki, S., Campos, E., Chambers, D., Feely, R.A., Gulev, S., Johnson, G.C., Josey, S.A., Kostianoy, A., Mauritzen, C., Roemmich, D., Talley, L.D., and Wang, F., 2013. Observations: Ocean. In: Climate Change 2013: The Physical Science Basis. Contribution of Working Group I to the Fifth Assessment Report of the Intergovernmental Panel on Climate Change [Stocker, T.F., Qin, D., Plattner, G.-K., Tignor, M., Allen, S.K., Boschung, J., Nauels, A., Xia, Y., Bex, V., and Midgley, P.M. (eds.)]. Cambridge University Press, Cambridge, United Kingdom and New York, NY, USA.

Salt, L.A., Thomas, H., Prowe, A.E.F., Borges, A.V., Bozec, Y., de Baar, H.J.W., 2013. Variability of North Sea pH and CO_2 in response to North Atlantic Oscillation forcing. J. Geophys. Res. Biogeosci. 118 (1-9), 2013. http://dx.doi.org/10.1002/2013JG002306.

Salt, L.A., Thomas, H., Bozec, Y., Borges, A.V., de Baar, H.J.W., 2015. The internal consistency of the North Sea carbonate system. J. Mar. Syst. (in revision).

Sarmiento, J.L., Gruber, N., 2006. Ocean Biogeochemical Dynamics. Princeton University Press, pp. 332–333.

Schiettecatte, L.S., Thomas, H., Bozec, Y., Borges, A.V., 2007. High temporal coverage of carbon dioxide measurements in the Southern Bight of the North Sea. Mar. Chem. 106, 161–173.

Schwichtenberg, F., 2013. Drivers of the carbonate system variability in the Southern North Sea: River input, anaerobic alkalinity generation in the Wadden Sea and internal processes Ph.D. thesis University of Hamburg.

Takahashi, T., Broecker W.S., Werner S.R. and Bainbridge, A.E., 1980. Carbonate chemistry of the surface waters of the world oceans, in Isotope Marine Chemistry, edited by E.D. Goldberg, Y. Horibe and K. Saruhashi, pp. 291-326, Uchinda Rokakuho Pulb. Co. Ltd. Tokyo.

Takahashi, T., Sutherland, S.C., Sweeney, C., Poisson, A., Metzl, N., Tilbrook, B., Bates, N., Wanninkhof, R., Feely, R.A., Sabine, C., Olafsson, J., Nojiri, Y., 2002. Global sea-air CO_2 flux based on climatological surface ocean pCO_2, and seasonal biological and temperature effects. Deep-Sea Res. II 49, 1601–1622.

Thomas, H., Schneider, B., 1999. The seasonal cycle of carbon dioxide in Baltic Sea surface waters. J. Mar. Syst. 22, 53–67.

Thomas, H., Bozec, Y., Elkalay, K., de Baar, H.J.W., 2004. Enhanced open ocean storage of CO_2 from shelf sea pumping. Science 304, 1005–1008.

Thomas, H., Bozec, Y., Elkalay, K., de Baar, H.J.W., Borges, A.V., Schiettecatte, L.-S., 2005a. Controls of the surface water partial pressure of CO_2 in the North Sea. Biogeosciences 2, 323–334.

Thomas, H., Bozec, Y., de Baar, H.J.W., Elkalay, K., Frankignoulle, M., Schiettecatte, L.-S., Kattner, G., Borges, A.V., 2005b. The Carbon Budget of the North Sea. Biogeosciences 2, 87–96.

Thomas, H., Prowe, A.E.F., van Heuven, S., Bozec, Y., de Baar, H.J.W., Schiettecatte, L.-S., Suykens, K., Koné, M., Borges, A.V., Lima, I.D., Doney, S.C., 2007. Rapid decline of the CO_2 buffering capacity in the North Sea and implications for the North Atlantic Ocean. Glob. Biogeochem. Cycles 21, GB4001. http://dx.doi.org/10.1029/2006GB002825.

Thomas, H., Prowe, A.E.F., Lima, I.D., Doney, S.C., Wanninkhof, R., Greatbatch, R.J., Schuster, U., Corbière, A., 2008. Changes in the North Atlantic Oscillation influence CO_2 uptake in the North Atlantic over the past 2 decades. Glob. Biogeochem. Cycles 22, GB4027. http://dx.doi.org/10.1029/2007GB003167.

Tsunogai, S., Watanabe, S., Sato, T., 1999. Is there a "continental shelf pump" for the absorption of atmospheric CO_2? Tellus 51B, 701–712.

Wakelin, S.L., Holt, J.T., Blackford, J.C., Allen, J.I., Butenschön, M., Artioli, Y., 2012. Modeling the carbon fluxes of the northwest European continental shelf: Validation and budgets. J. Geophys. Res. 117, C05020. http://dx.doi.org/10.1029/2011JC007402.

Winkler, L.W., 1888. Die Bestimmung des im Wasser gelösten Sauerstoffes. Chem. Ber. 27, 2843–2855.

Wootton, J.T., Pfister, C.A., Forester, J.D., 2008. Dynamic patterns and ecological impacts of declining ocean pH in a high-resolution multi-year dataset. PNAS 105 (48), 18848–18853.